Fall 1983

Application of Ground Penetrating Radar to the Detection of Subsurface Cavities

Gary L. Kuhns
University of Central Florida

APPLICATION OF GROUND PENETRATING RADAR TO THE DETECTION OF SUBSURFACE CAVITIES

BY

GARY L. KUHNS
B.S.E., University of Central Florida, 1982

THESIS

Submitted in partial fulfillment of the requirements
for the degree of Master of Science in Engineering
in the Graduate Studies Program of the College of Engineering
University of Central Florida
Orlando, Florida

Fall Term
1983

ABSTRACT

Ground Penetrating Radar (GPR) identifies subsurface features by distinguishing materials with different dielectric constants and electrical conductivities. Subsurface cavities can, therefore, be detected by the variation in their electrical properties from the electrical properties of the surrounding material. To test the cavity detection ability of GPR, subsurface cavities of varying size, shape and content were modeled. Radar response to the cavity models was found to be affected by the composition of the surrounding soil material, the depth of the groundwater table, and the radar signal frequency.

Based on knowledge gained from the cavity modeling study, a natural subsurface cavity was identified during a GPR field investigation. Limestone features such as bedding planes and fractures were mapped, and a detailed lake bottom profile was obtained by the radar system.

ACKNOWLEDGEMENTS

The writer wishes to express his appreciation to his major professor, Dr. Shiou-San Kuo, for his guidance and encouragement during this study. He would also like to extend his gratitude to Jim Doolittle, of the U.S. Soil Conservation Service, for generously sharing his time and equipment. He is also grateful to Mike Tannous for his hard work in helping to collect the radar data, Lawrence Kuhns and John Kuhns for their contributions toward the data collection phase of this project, and Lynn Hauman for drafting many of the diagrams in this paper. Many thanks are also due the College of Engineering and the Department of Civil Engineering and Environmental Sciences for the EIES grant which made this research possible, and to Dr. Wanielista and Dr. Carroll for reading the draft version of this thesis. In addition, the author wishes to express his appreciation for being selected as the F. Hubbard Scholar during his graduate work at UCF.

TABLE OF CONTENTS

LIST OF FIGURES

LIST OF FIGURES (Continued)

LIST OF TABLES

NOMENCLATURE

Symbol	Description
r	energy reflection coefficient
E_r	reflected pulse energy
Eo	incident pulse energy
V	velocity
c	propagation velocity in free space, 1 ft/ns
R	depth to target
twt	two-way pulse travel time
TPL	total power loss
PF	performance figure
G	antenna gain
a	target cross section
f	frequency
ω	$2\pi f$
λ	signal wave length
ε_r	relative dielectric constant
ε_o	permittivity constant, 8.85×10^{-12}, farad/meter
μ_o	permeability constant, $4\pi \times 10^{-7}$, henry/meter
μ_r	relative permeability, 1

CHAPTER I

INTRODUCTION

Subsurface cavities are an integral part of the Central Florida environment. Due to the existing combination of hydrologic and geologic conditions, cavity formations are common throughout the area. When these subsurface cavities collapse, a depression forms on the ground surface commonly known as a "sinkhole". Many of the natural lakes and ponds which are so numerous in Central Florida were formed by sinkhole collapse.

In recent years, however, sinkhole formation in urban areas has become a serious problem. The Winter Park Sinkhole is probably the best known collapse of this kind. This 320 foot diameter sinkhole consumed almost two acres of land and destroyed millions of dollars worth of property. Although the Winter Park Sinkhole is an extreme example, it demonstrates the destruction which is possible when a subsurface cavity collapses in a developed area.

A quick, inexpensive, subsurface exploration method is needed which can detect cavities over a large area prior to development. Presently, boreholes are drilled at a survey site to determine the subsurface conditions. However, because information is only provided at the specific points where the boreholes are drilled, many boreholes are needed to determine if there are any subsurface cavities

at the site. Because drilling is time-consuming and expensive, it is usually impractical to drill enough holes to rule out the presence of cavities.

Subsurface exploration techniques which can distinguish different earth materials by their physical properties are known as geophysical methods. These methods can identify subsurface features without expensive drilling or excavation. There are many geophysical methods which can be applied to cavity detection. Gravity, seismic, electrical resistivity, magnetic and electromagnetic techniques have all been tested with varying levels of success. Although none of the geophysical methods can be applied successfully to every subsurface condition, the electromagnetic method known as Ground Penetrating Radar (GPR) is a practical and versatile exploration method and a potentially effective cavity detection technique.

One objective of this study is to evaluate the ability of GPR to detect the presence of subsurface cavities. Another objective is to gain an insight into the interpretation of the radar signals reflected from these cavities. In order to achieve these goals, subsurface cavities are modeled to test the GPR equipment under simulated conditions. By acquiring the radar data under known conditions, the radar signals reflected from the modeled cavities can be correlated with the actual cavity properties such as location, depth, size, shape and contents. This knowledge of the radar response to varying cavity conditions can serve as an aid in the interpretation of radar data acquired during actual field investigations.

CHAPTER II

LITERATURE REVIEW

Ground penetrating radar systems in their present form have been in use since 1970. Ulriksen (1982) estimates that about 87 articles have been written on the subject of GPR since that time. The bulk of these articles cover such topics as soil profiling, rock exploration and pavement and bridge evaluation. Relatively few articles, however, deal directly with cavity detection. Inexperience in interpreting field data, and depth limitations of the radar signal make cavity detection difficult in many cases. However, the development of interpretive skills and sophistication of the radar equipment will make cavity detection more practical in the near future. The following literature review provides a general summary of GPR applications in the area of cavity detection.

In May 1974, ground penetrating radar experiments were sponsored by the National Coal Board of Great Britain (Cook 1974). The purpose of these experiments was to evaluate the ability of GPR to detect unmapped abandoned mine shafts ahead of present mining activities. These shafts can contain mud and water under pressure which could pose a serious safety hazard. The experiments were conducted with the radar equipment located in the mine. A 100 MHz radar antenna was coupled directly to the rock surface to reduce the radar

signal attenuation. By employing this method, researchers were able to obtain clear reflections from interfaces through up to 28 feet of coal.

Moffat and Puskar (1976) used a pulse radar system to locate abandoned coal mines near Lake Hope in Ohio. Drainage from the mines was polluting Lake Hope and one solution to the problem was to seal the mine entrances and to flood the mine. However, it was unknown if the coal at the front of the seam and between tunnels was thick enough to withstand the pressure of the entrapped water. Radar probings were conducted on the hill above the coal seam to locate tunnels. If tunnel detection proved possible, the thickness of the coal pillars between tunnels could be determined.

A very low frequency 10 MHz signal was used in the investigation. The tunnel which was investigated measured about 4 feet from roof to floor and was about 12 feet wide. The overburden consisted mostly of sandstone and a thin layer of topsoil. The pulse velocity in the sandstone was measured to be 0.3 feet per nanosecond which corresponds to a dielectric constant of about 9. The tunnel in the coal seam was successfully detected at a depth of 19 feet.

Dolphin, Beatty, and Tanzi (1978) conducted a radar investigation of a mountain in New Mexico known as Victorio Peak. The geology of the mountain includes many interesting subsurface features such as cracks, fissures, cavities, caves, and tunnels. The radar system used in the investigation was capable of operating at frequencies of 20, 25, 50, 80 and 125 MHz. The propagating medium was primarily limestone-based.

The radar system was successfully used to measure the thickness of cave-ins, roof thicknesses over known underground chambers, and other subsurface features at depths ranging from 10 to 50 feet. During the investigation, echoes at great depths, with a total time delay of 1600 to 2500 nanoseconds, continued to recur. Numerous probings from several locations appeared to verify the existence of radar reflections which were occurring at depths from 350 to 431 feet. It is believed that these echoes were reflected from very large caverns within the mountain. The ability of the radar signal to penetrate to such great depths is credited to the enormous size of the caverns and the low signal attenuation in the propagating medium.

One way of overcoming the depth limitations of the radar signal is to place the antenna in a probe that can be lowered into a borehole. S.A. Suhler (1981), a researcher for the Southwest Research Institute, developed a borehole probe that could be used to locate cavities and unstable roof conditions ahead of mining activities. The purpose of acquiring this data was to prevent mining accidents.

Suhler developed a 100 MHz radar probe which both transmitted and then received the radar signals after they were reflected from interfaces around the borehole. The probe successfully located a known abandoned mine at the Kemmerer Coal Company at Kemmerer, Wyoming. The mine was 35 feet deep and located horizontally 50 feet from the borehole. However, at the York Canyon Mine in Raton, New Mexico, attempts to locate a mine shaft and a fault line at distances

of 50 feet were unsuccessful. At both test sites, coal was the medium being surveyed. In a hard rock medium, Suhler was able to distinguish reflections from geologic structures at distances of 60 feet using computer processing techniques to reduce signal clutter.

Thomas E. Owen (1981), also of the Southwest Research Institute, used a hole-to-hole method to locate cavities. This method incorporates separate transmitter and receiver probes which allow radar pulses to be sent from one hole to another. This sytem is illustrated in Figure 1. Because electromagnetic waves travel faster through an air-filled cavity than through the surrounding earth, it is possible to distinguish their presence by a decrease in the pulse travel time between probes in the cavity area. Furthermore, the boundaries and the geometric shape of the cavity diffract and scatter the transmitted pulse causing disturbances in the wave pattern which can be seen by the receiving probe.

The equipment for Owen's testing included receiver and transmitter probes with a frequency of 100 MHz, a dual-drum wireline winch that could be used to raise and lower the transmitter and receiver probes simultaneously or separately, a control unit, and a magnetic tape recorder. The first test area was Medford Cave near Gainesville, Florida. This cave is a shallow limestone solution cavity, with narrow caverns 3 meters to 12 meters long. The depth of the cave ranges from 5 to 20 meters. Results of the borehole probe showed strong verification of subsurface cavities. Another test site was the Colorado School of Mines Test Site at Idaho

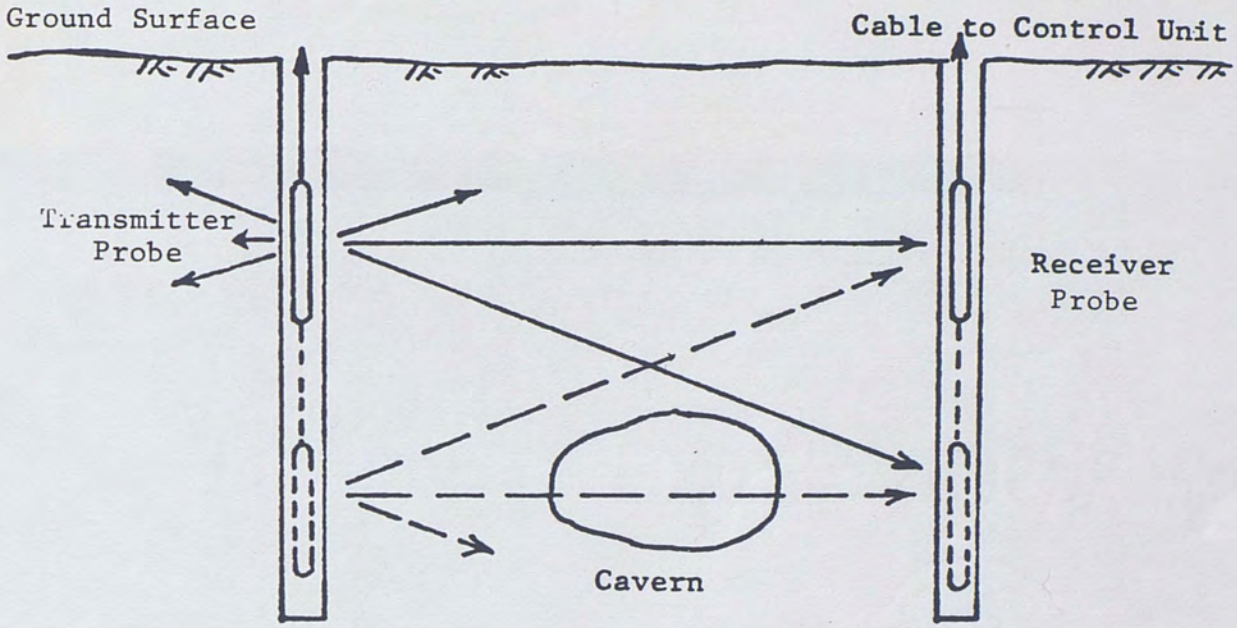

Fig. 1. Hole-to-hole radar system.

Springs, Colorado. The tunnel was located by the radar system at a depth of 48.5 meters. The results of these tests indicate a strong potential for the ability of a hole-to-hole radar system to locate subsurface cavities.

James Doolittle (1982) tested GPR's ability to locate areas of subsurface fracturing and cavitation in the limestone bedrock

areas of the Texas-Oklahoma region. His testing was performed with the radar antenna located on the ground surface. Antenna frequencies of 120 MHz, 300 MHz and 500 MHz were used. In most cases, the results were disappointing. The high conductivity of the overburden soils caused a rapid attenuation of the radar signal which severely restricted the probing depth. Even when using the lower frequency antennas, which provide the deepest penetration, probing depths were limited to about 8 meters. Although attempts at locating deep cavities were unsuccessful, the GPR system did provide a high quality record of shallow subsurface features in the limestone bedrock such as fracture zones and bedding planes.

Peter Ulriksen (1982), of Lund University in Sweden, used a GSS radar system to detect caves in limestone near Ignaberga, Sweden. The limestone was covered by till and the groundwater level was well below the cave elevation. The cave reflection patterns are the small hyperbolic dark bands shown in Figure 2. Because no drillings were performed to determine the actual cave depth, the depths were estimated by approximating the pulse velocity. Based on a dielectric constant of 9 in the dry till overburden, and a dielectric constant of 4 for the equally dry limestone, the left cavity was determined to be 10.7 meters deep. The two reflections from the cavity on the right are believed to come from the roof and floor of the cave. The cave height is about 7.4 meters.

Ulriksen studied another cave south of Visby on Gotland, Sweden. This cave descends at a 28 degree angle from the ground surface, and

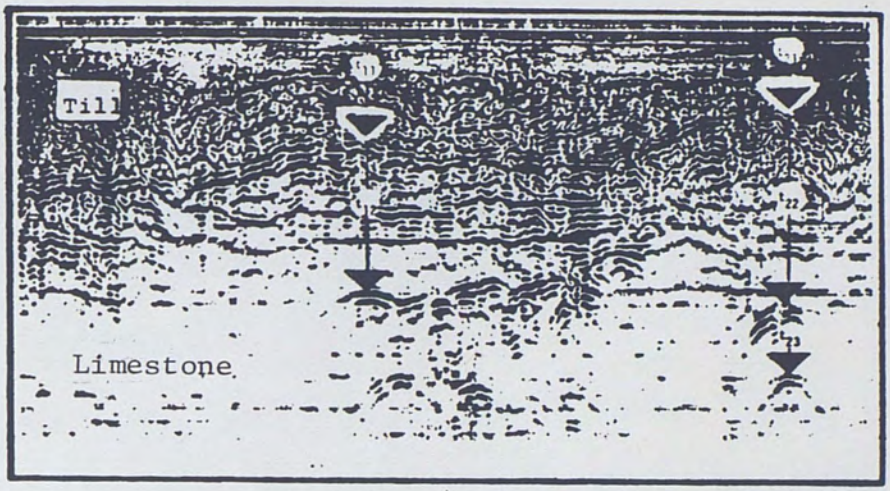

Fig. 2. Radar profile showing cavities in limestone (Ulriksen 1982).

measures 0.75 meters from roof to floor. Because there was no soil cover at this location, the antenna was dragged directly over the limestone surface. Five traverses were made perpendicular to the length of the cave using a 300 MHz antenna.

The resulting radar data is shown in Figure 3. Reflections from the cave interfaces are labeled I and II, and the three horizontally layered interfaces are labeled A, B, and C. The five traverses are labeled L_1 through L_5 and the depth to the cave roof increases with each successive traverse. The results indicate very

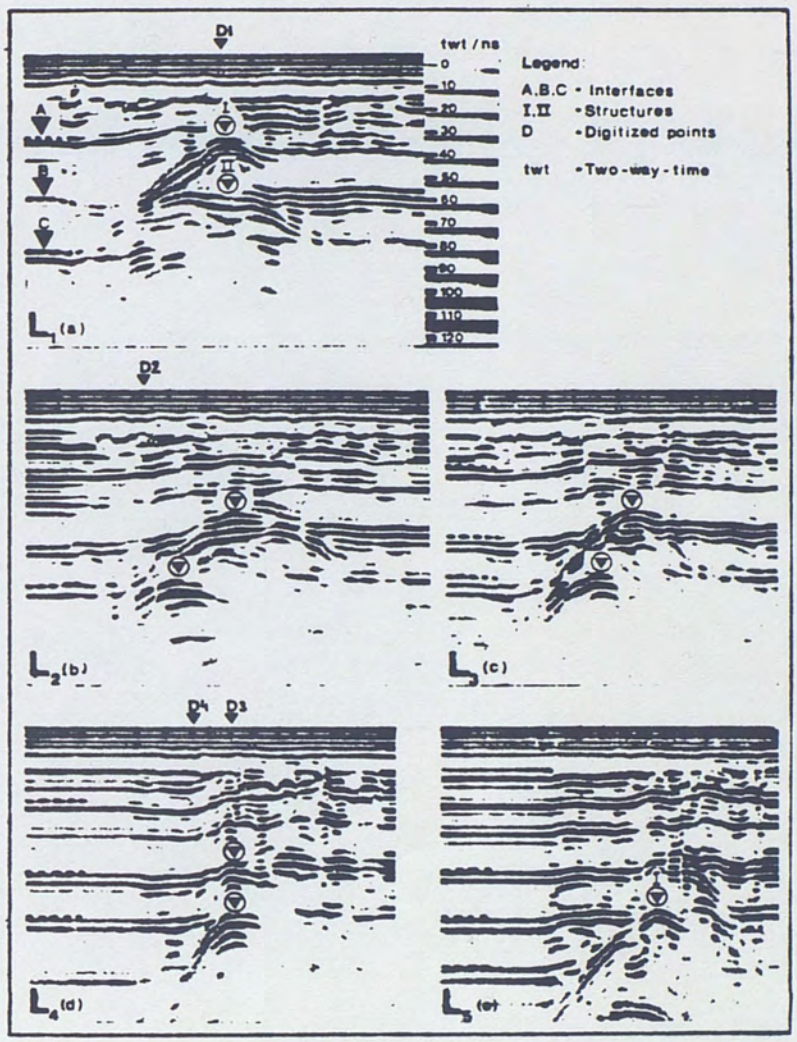

Fig. 3. Radar records from five cavity profiles (Ulriksen 1982).

strong reflections from the roof and floor of the air-filled cave. However, an analysis of the reflected signal amplitudes and travel times indicates that the oscillations in the reflection from the roof overlap the reflection from the floor. This is due to the close spacing of the two interfaces. Because of this overlapping, reflection II cannot be considered a unique reflection from the cave floor.

In summary, Ground Penetrating Radar has been applied to the detection of subsurface cavities over the past 10 years with varying degrees of success. The success of the radar method is primarily dependent on the subsurface conditions at the investigation site. The best results are obtained in dry rock or dry sand mediums of low conductivity. Much more research is necessary to determine the ability of GPR to detect cavities in areas of karst topography, such as Central Florida.

CHAPTER III

GROUND PENETRATING RADAR THEORY AND OPERATION

Electromagnetic Principles

Ground Penetrating Radar is the latest technological advance in geophysical exploration. A GPR system provides a graphic record of subsurface features without disturbing the material being probed. Although the system is technically complex, its operation is based on fundamental principles of electromagnetic wave theory.

When an electromagnetic pulse traveling through a medium strikes another medium with different electrical properties, part of the pulse is reflected and the rest of the pulse continues to travel through the new medium. The reflected pulse energy, E_r, from an interface between two materials is related to the incident energy, E_o, by the relationship:

$$r = \frac{E_r}{E_o} = \frac{1 - (\varepsilon_2/\varepsilon_1)^{\frac{1}{2}}}{1 + (\varepsilon_2/\varepsilon_1)^{\frac{1}{2}}} \qquad (1)$$

where:

r = the reflection coefficient at the interface between materials 1 and 2

$\varepsilon_1, \varepsilon_2$ = the relative dielectric constants for materials 1 and 2, respectively

The dielectric constant is a measure of the electrical storage capacity of a material. If material 2 has a higher dielectric constant

than material 1, the reflection coefficient will be negative. Therefore, the pulse reflected from the interface will have a polarity opposite to the transmitted pulse. Also, if the dielectric constant of material 2 varies greatly from the dielectric constant of material 1, most of the incident energy will be reflected. Conversely, if material 2 has a dielectric constant about the same as material 1, most of the incident energy will be transmitted through the interface.

The GPR system uses this electromagnetic principle to obtain a profile of subsurface features. The antenna, located on the ground surface or in a borehole, transmits a radar pulse into the earth or other media to be tested. When the pulse strikes an interface between two subsurface materials with different dielectric constants, some of the pulse energy is reflected, and the remainder continues on through the new material to the next interface and so on. The reflected pulses from the different subsurface interfaces are received by the antenna and are processed to form a pattern of pulse reflection versus pulse travel time. The radar system can be thought of as a sophisticated timing device which emits an electromagnetic pulse and records the amount of time it takes the various interface reflections to return. By proper interpretation of the radar reflection data, the subsurface features of an area can be described.

Radar Equipment Function

The GPR equipment used in this study is shown in Figure 4. This equipment, which is manufactured by Geophysical Survey Systems,

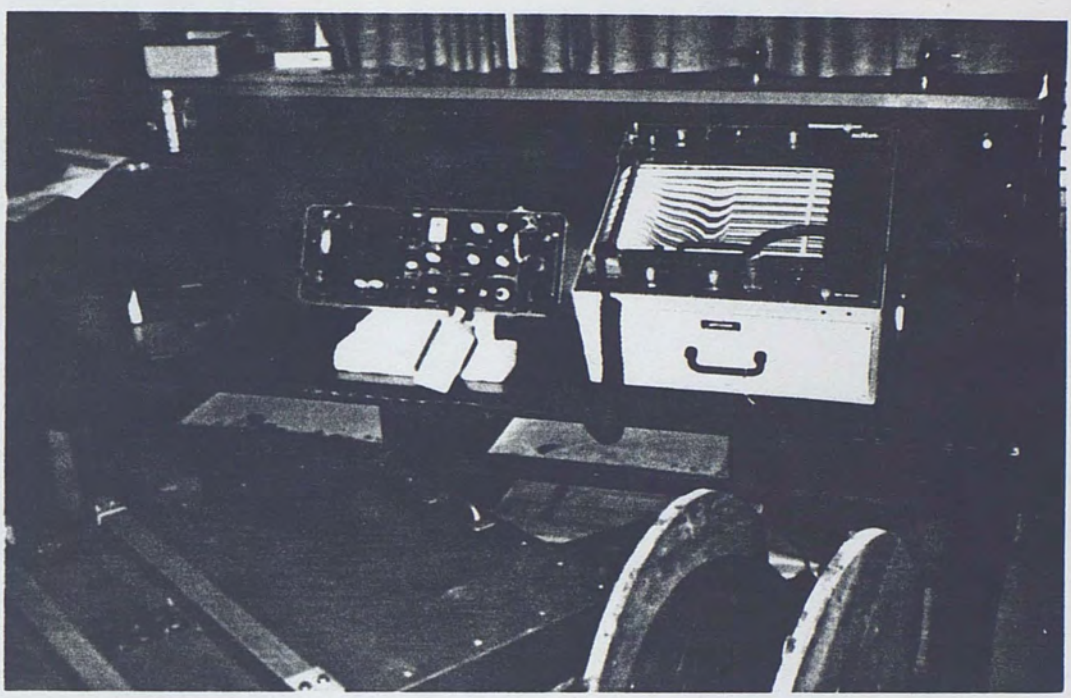

Fig. 4. Geophysical Survey Systems, Inc. radar unit.

Inc., includes several transmitter/receiver antennas of varying frequencies, a radar control unit, and a graphic recorder. Figure 5 shows the GPR system in block diagram and functional form. The power supply furnishes a DC voltage to the pulse transmitter. The transmitter uses a fast-acting switch to create a time-limited signal, or voltage pulse, which is sent directly to the broadband antenna during

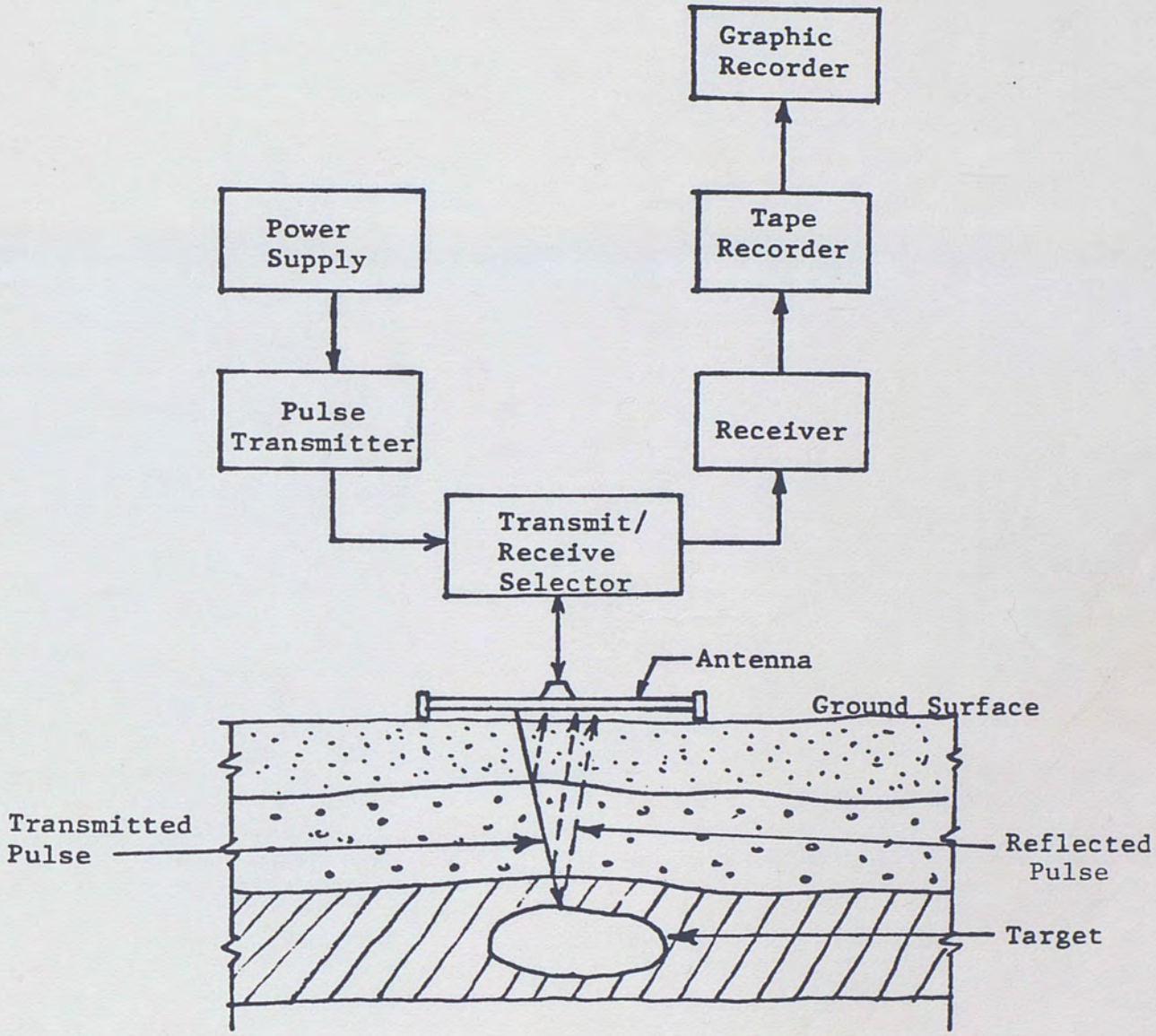

Fig. 5. GPR system in block diagram and functional form (Morey 1974).

the transmit cycle. This pulse is a brief electromagnetic transient shaped to quasi-gaussian form. The transmitted pulse travels through the subsurface until it reaches an interface as shown in Figure 5. The signals reflected by the interface are received by the same antenna which is used for transmission by using a transmit-receive selector that prevents transmitted pulses from entering and damaging the receiver. The receiver system amplifies the received reflections and uses a time-domain sampling technique to construct a waveform of similar shape to that of the actual received signal, but with a much longer time base. The resulting frequency is in the audio range where it can be readily recorded, processed, and displayed.

The purpose of the control unit is to allow the operator to amplify the reflected waveform as desired and to adjust the time span, or probing depth, of the radar scan. The time span is determined by the range adjustment. The calibration charts for this adjustment are shown in the Appendix. An oscilloscope on the control unit displays a trace of the reflected waveform so that it can be processed as desired by the operator. After being processed by the control unit, the waveform is sent to the graphic recorder for a hardcopy display. The graphic recorder produces an image by printing strong signals as black and weak signals as white. Signals of intermediate strength are printed in varying shades of gray.

As the antenna is pulled along the ground surface, a continuous stream of reflected waveforms is processed by the control unit and

instantly sent to the graphic recorder. A subsurface profile is developed as the waveforms are printed by the graphic recorder. This process creates a continuous record of subsurface reflections over a given survey distance from which subsurface features, such as soil layers, rock layers, and pipes, can be distinguished.

Interpretation of Radar Data

An example of a simple reflection pattern and the corresponding graphical record is shown in Figure 6. The time scale, or depth scale, of the scan is in the downward vertical direction. The strength of the received signals is shown by the size of the waveform in the signal pattern on the left, and by the intensity of the dark bands on the graphical record.

The received signal pattern consists of three basic parts: (1) the transmit pulse, (2) the surface reflection, and (3) the reflection from a subsurface interface, such as a soil layer. The first dark band at the top of the profile is the transmit pulse. This pulse is a feed-through of the transmitted pulse directly into the receiver section of the antenna and serves as a time reference. The group of closely spaced dark bands immediately following the transmit pulse is the strong reflection from the surface. Then at a point on the time scale equal to the pulse travel time from the antenna to the interface and back to the antenna, the interface reflection appears.

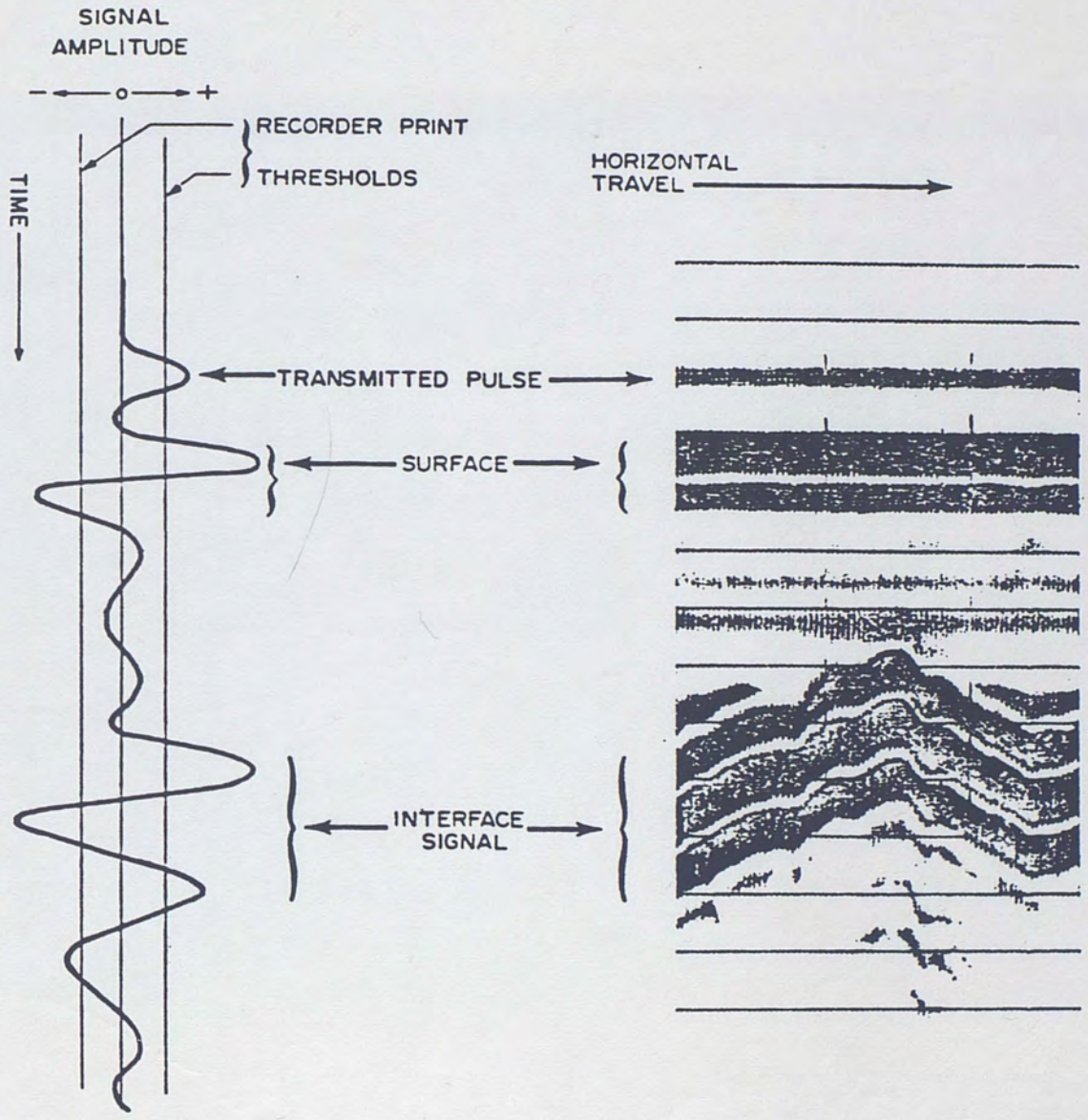

Fig. 6. Typical signal pattern (left) and corresponding graphical record (GSSI, 1982).

An important characteristic of the reflection pattern is the appearance of three dark bands in the reflection from the interface instead of just one. This triple band, which is typical of all radar data, is caused by oscillations in the reflection of the pulse. This oscillation reduces the ability of the system to discriminate between closely spaced interfaces. If a second interface close to the first interface generates a pulse reflection, that reflection will superimpose itself onto the oscillations from the pulse reflection from the first interface. If the superimposing waveforms have the same polarity, or sign, they will be additive, and if their polarity is opposite, they will tend to cancel each other out. However, the lower interface will not be completely obscured because portions of its own oscillations will appear, but the actual depth of the lower interface will be difficult to determine. For instance, if a thin clay layer surrounded on top and bottom by sand is being surveyed, the depth to the clay layer can easily be determined but superposition of the waveforms from the top and bottom interfaces will make the thickness difficult to estimate.

The radar antenna radiates signals into the ground in a beam roughly conical in shape. The included angle of the beam from front to back is approximately 90 degrees, and the side beam angle is about 60 degrees. An important feature to recognize when interpreting radar data is that the antenna only receives reflected pulses from an interface when the transmitted pulse strikes the interface at a 90 degree angle. In other words, the radar system

only sees subsurface features which are normal to some portion of the conical radiation pattern. When an interface is planar and parallel to the path of the antenna, such as a soil layer, only the pulse energy directed straight down is reflected back to the antenna. In other words, at any one moment the antenna only "sees" the portion of the flat soil layer directly beneath it.

For interfaces with a curved surface, such as a pipe, the reflection pattern is quite different. The surface of a round pipe is normal to the conical radiation beam at many antenna locations on the ground surface. As shown in Figure 7, as the antenna moves toward the pipe, the first reflection is received when the antenna is at a 45 degree angle from a vertical line drawn through the center of the pipe. Reflections from the pipe continue to be received until the antenna reaches the same horizontal distance, X, on the other side of the pipe. A continuous record obtained in this manner will produce a hyperbolic travel time curve as shown in Figure 7. The "tails" of the hyperbola represent reflections from the pipe when the antenna is not directly overhead and, therefore, "sees" the pipe as being deeper than it actually is. The apex of the hyperbola represents the true pipe depth. This radar response is typical for all curved interfaces and must always be considered when interpreting radar data. The reflection from the bottom of a circular pipe will have the same hyperbolic shape as the reflection from the top. This is because the shortest pulse travel distance to the pipe bottom will also occur when the antenna is directly above the center of the pipe.

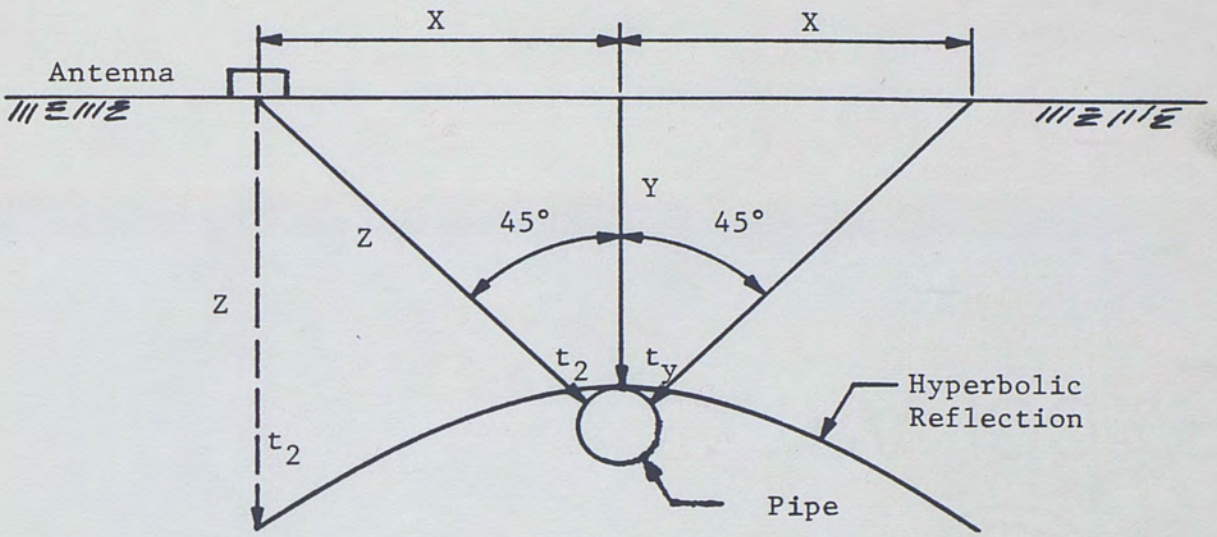

Fig. 7. Hyperbolic reflection from a circular pipe.

Depth Calibration

Because the radar system provides a record of interface reflections versus pulse travel time, the depth to a subsurface interface can be determined if the velocity of the radar pulse through the propogating material is known. This velocity is related to the dielectric constant of the medium by the relationship:

$$V = \frac{C}{(\varepsilon_r)^{\frac{1}{2}}} \qquad (2)$$

where:

C = propagation velocity in free space (approximately 1 foot per nanosecond)

ε_r = relative dielectric constant of medium

Once the dielectric constant of the subsurface material is determined, the pulse velocity can be calculated from equation 2. However, the electrical parameters of earth material, dielectric constant and conductivity, are difficult to estimate because they are dependent upon the water content, temperature, pressure, and impurities of the material, and the frequency of the radar signal (Morey 1974). Approximate values of dielectric constant and conductivity for various earth materials are given in Table 1. These values are based on typical natural conditions of temperature and pressure, and the operating frequency range of the radar signal.

The water content of an earth material has a very significant effect on its electrical parameters. Increasing water content tends to increase the dielectric constant of a material. An increase in the dielectric constant causes a decrease in the pulse velocity. This phenomenon is important to consider when probing at depths below the groundwater table. Because the pulse velocity will decrease when the pulse reaches the saturated soil below the groundwater table, the depth scale of the radar record will be elongated.

The conductivity of an earth material also increases with increasing moisture content, and the amount of salts in solution. The maximum penetration depth of the radar signal is highly dependent on the material conductivity.

TABLE 1

APPROXIMATE VHF ELECTROMAGNETIC PARAMETERS
OF TYPICAL EARTH MATERIALS*

Material	Approximate Conductivity σ (mho/cm)	Approximate Dielectric Constant, ε_r
Air	0	1
Fresh Water	10^{-4} to 3×10^{-2}	81
Sea Water	4	81
Sand "dry"	10^{-7} to 10^{-3}	4 to 6
Sand, saturated (fresh water)	10^{-4} to 10^{-2}	20
Silt, saturated (fresh water)	10^{-3} to 10^{-1}	30
Clay, saturated (fresh water)	10^{-1} to 1	40
Dry, sandy, flat coastal land	2×10^{-3}	10
Rich agricultural land low hills	10^{-2}	15
Fresh water ice	10^{-4} to 10^{-2}	4
Permafrost	10^{-5} to 10^{-2}	4 to 8
Granite (dry)	10^{-8}	5
Limestone (dry)	10^{-9}	7

* Data from Von Hippel (1954), Kraichmann (1970), and Wait (1971).

The most accurate way of determining the pulse velocity is to scan over a target of known depth, such as a pipe or a soil layer. By obtaining the two-way travel time of the reflected pulse from the radar record, the pulse velocity may be calculated from:

$$V = \frac{2R}{twt} \qquad (3)$$

where:

R = measured depth to target

twt = two-way travel time of pulse

The pulse velocity obtained by this method is an average velocity for the material between the surface and the target. It is valid if the area being surveyed has subsurface conditions similar to the target site. However, this average velocity might not be valid at depths greater than the target depth due to possible changes in earth material or water content. It is essential that accurate subsurface information be obtained by sample borings in order to reasonably estimate the depth scale of the radar data.

Another method of obtaining average pulse velocity is described in the Geophysical Survey Systems, Inc. SIR (Subsurface Interface Radar) Manual (1982). This method is based on the previously discussed concept of radar reflections from a pipe. Referring to Figure 7, the first reflection from the pipe will be recorded at a slant distance, Z, corresponding to a two-way travel time, t_z. This depth is greater than the actual depth to the pipe, Y,

corresponding to the time, t_y. It must be assumed that the subsurface material above the pipe is homogeneous. Also, the pipe dimensions must be insignificant relative to the pipe depth and the horizontal distance, X. Using the following geometrical relationships:

$$X^2 + Y^2 = Z^2 \tag{4}$$

and

$$\frac{ty}{tz} = \frac{Y}{Z} \tag{5}$$

The depth to the pipe is derived as:

$$Y = \frac{X}{\left[\left(\frac{tz}{ty}\right)^2 - 1\right]} \tag{6}$$

Penetration Depth of Radar Signal

The effectiveness of a GPR survey is limited in many cases by the penetration depth of the radar signal. The maximum penetration depth of the radar pulse is determined by limitations of the radar equipment and by propagation losses in the material being probed. In order to detect a pulse reflected from a subsurface interface, the total propagation loss must be less than or equal to the performance figure of the radar equipment,

$$TPL \leq PF \tag{7}$$

where the performance figure, PF, of the radar system is defined as:

$$PF = \frac{\text{radiated peak power}}{\text{minimum detectable received signal power}} \qquad (8)$$

The PF is limited by practical considerations in the design of the radar equipment. Presently, radar performance figures are typically limited to 100 to 110 db, but improved designs should make PF's on the order of 200 to 230 db possible in the future (Cook 1981).

The total propagation loss, TPL, is defined as:

$$TPL = \text{spreading loss} + \text{propagation loss} \qquad (9)$$

The spreading loss is a decrease in the energy density of the radar signal which is caused by the increasing area of the radar beam as it travels through the medium. The fraction of the transmitted signal which reaches the subsurface interface, or target, can be expressed as:

$$\frac{\text{outgoing power spread area}}{\text{target cross-section}} = \frac{4\pi R^2/G}{a} \qquad (10)$$

where:

R = depth to target

G = antenna gain

a = target cross-section

The fraction of the power reflected from the target which is received by the antenna is defined by:

$$\frac{\text{returning power spread area}}{\text{receiving antenna effective area}} = \frac{4\pi R^2}{G\lambda^2/4\pi} \qquad (11)$$

where:

λ = radar signal wavelength

The product of these two factors yields:

$$\text{total spreading loss} = \frac{64\pi^3 R^4}{aG^2\lambda^2} \qquad (12)$$

This expression shows that the spreading loss increases rapidly with increasing target depth. However, increases in target cross-section area, antenna gain, and signal wavelength will decrease spreading loss. Due to this relationship, low frequency antennas, which generate larger signal wavelengths, will incur somewhat smaller spreading losses than higher frequency antennas.

The absorption loss is expressed by the absorption coefficient, α, of the medium being probed. This coefficient can be calculated from the theoretical formula:

$$\alpha = w\left\{\frac{\mu\varepsilon}{2}\left[\left(1 + \frac{\sigma^2}{w^2\varepsilon^2}\right)^{\frac{1}{2}} - 1\right]\right\}^{\frac{1}{2}} \qquad (13)$$

where:

$w = 2\pi f$ (radians/second)

$\mu = \mu_o \mu_r = 4\pi \times 10^{-7}$ (henry/meter)

$\varepsilon = \varepsilon_o \varepsilon_r = 8.85 \times 10^{-12} \varepsilon_r$

σ = conductivity (mhos/meter)

The absorption coefficient can be conveniently expressed in terms of attenuation, A, in decibels per meter by the following expression:

$$A = 12.863 \times 10^{-8} f(\varepsilon_r)^{\frac{1}{2}} \left[\left(1 + \frac{\sigma^2}{w^2 \varepsilon^2}\right)^{\frac{1}{2}} - 1\right]^{\frac{1}{2}} \qquad (14)$$

Where f is the frequency and the other parameters are previously defined. From this relationship it can be seen that an increase in conductivity will cause a significant increase in signal attenuation. Due to this characteristic, earth materials with a high water content, and, therefore, a high conductivity, will attenuate the radar signal more rapidly than dry earth materials. Furthermore, an increase in frequency will also increase the signal attenuation. For this reason, low frequency antennas are used to achieve the greatest penetration depths. Table 2 lists attenuation values calculated by Morey (1974) for typical earth materials over the frequency range from 1 to 500 MHz. The attenuation values for sea water can be obtained by substituting the values of dielectric constant and conductivity from Table 1 into equation 14. The electrical parameters used to calculate attenuation for the other materials, however, are not known.

TABLE 2

ATTENUATION IN DECIBELS/METER*

Material	Frequency MHz			
	1	2	3	4
Pure water	0.025	0.039	0.408	16.191
Sandy soil (moist)	0.471	0.513	0.773	4.047
Clay soil (dry)	0.013	0.075	0.425	1.649
Clay soil (moist)	0.780	3.803	17.93	53.75
Sea water	34.50	108.54	326.54	592.03
Granite (dry)	0.732×10^{-5}	0.732×10^{-5}	0.732×10^{-5}	0.732×10^{-5}

* Data from Morey (1974).

The total attenuation loss for a signal reflected from a sub-surface interface is given by:

$$\text{attenuation loss} = 2AR \tag{15}$$

Therefore, the total power loss expressed in decibels is given by:

$$TPL = 10 \log_{10} \frac{64\pi^3 R^4}{aG^2\lambda^2} + 2RA \tag{16}$$

Using an analysis similar to the above, Cook (1981) calculated that penetration depths up to 100 meters may be possible under the

most favorable conditions in hard rocks, such as limestone and granite. He also stated that improvements in radar system design may make penetration depths up to 200 meters possible in the future.

Determination of the maximum penetration depth at a site before the actual radar survey is difficult due to the many factors which influence radar signal penetration. The electrical properties of soil, rock, and water vary greatly from site to site. Furthermore, under actual field conditions, the earth material being probed is most often non-homogeneous and the signal strength is quickly reduced due to the reflection of the signal from several layered interfaces. As seen from equation 16, the size and shape of the target will also affect the detection ability of the radar system.

Generally, penetration depths will be the greatest in low conductivity materials, such as ice, rock and sand, and the least penetration will be attained in high conductivity materials such as clay and sea water. Penetration depths of 230 feet have been reported in an Antarctic ice shelf, 75 feet in water saturated sands, 5 feet in wet clay, and less than a foot in sea water (Morey 1974). Clearly, a great deal remains to be learned about the performance of GPR. As use of the system becomes more widespread, data can be accumulated which will, hopefully, make GPR performance under given subsurface conditions more predictable.

CHAPTER IV

SUBSURFACE CAVITY MODELING AND RADAR PROFILING

In order to study the radar signal patterns reflected from subsurface voids, cavities of varying depth, size, shape and content were simulated. The cavity models were created by excavating to the desired depth, emplacing a lining or container, and backfilling with the excavated soil. The three model cavities buried above the water table were air-filled, and the single cavity placed below the water table was filled with water to simulate actual field conditions. Radar antennas with frequencies of 900, 500, 300 and 80 MHz were used to profile the cavity models.

The GPR cavity test site is located on the campus of the University of Central Florida. The soil at the site is primarily light tan, uniform, fine sand. The soil is classified SP in the Unified Soil Classification System or A-3 in the AASHTO system. At depths of 3.5 to 4 feet the sandy soil is interrupted by a layer of dark organic hardpan 1 to 2 feet thick. The water table is at a depth of approximately 4 feet.

Air-filled Cavities

As a preliminary test, an air-filled plastic cylinder was buried at a depth of 1.9 feet. The cylinder has a diameter of 11

inches and a length of 15 inches. It was placed on its side in the excavation and then covered as shown in Figure 8. Since this model cavity is relatively small in size and buried at a shallow depth, only high frequency antennas were used to obtain the best resolution. The antennas were pulled along a path perpendicular to the cylinder's length to profile a circular cross section of the cavity.

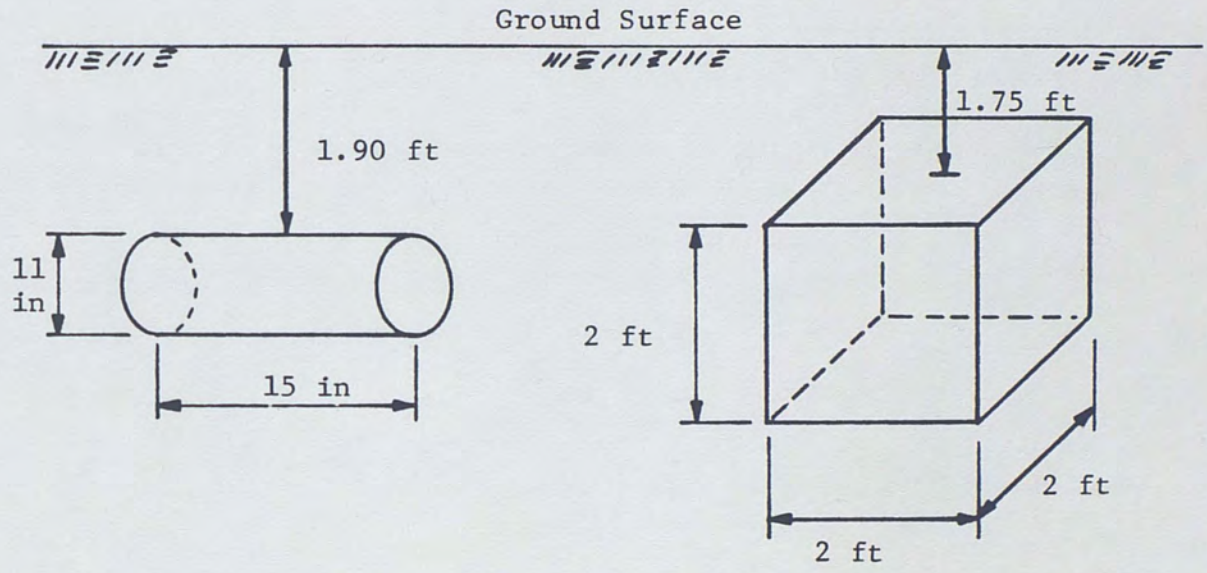

Fig. 8. Cylindrical and cubic air-filled cavities.

The radar profiles obtained with the 900 and 500 MHz antennas are shown in Figure 9 and 10, respectively. Referring to Figure 9, the two-way time scale in nanoseconds (ns) is shown on the right side of the radar profile. The total time span of 16.5 ns

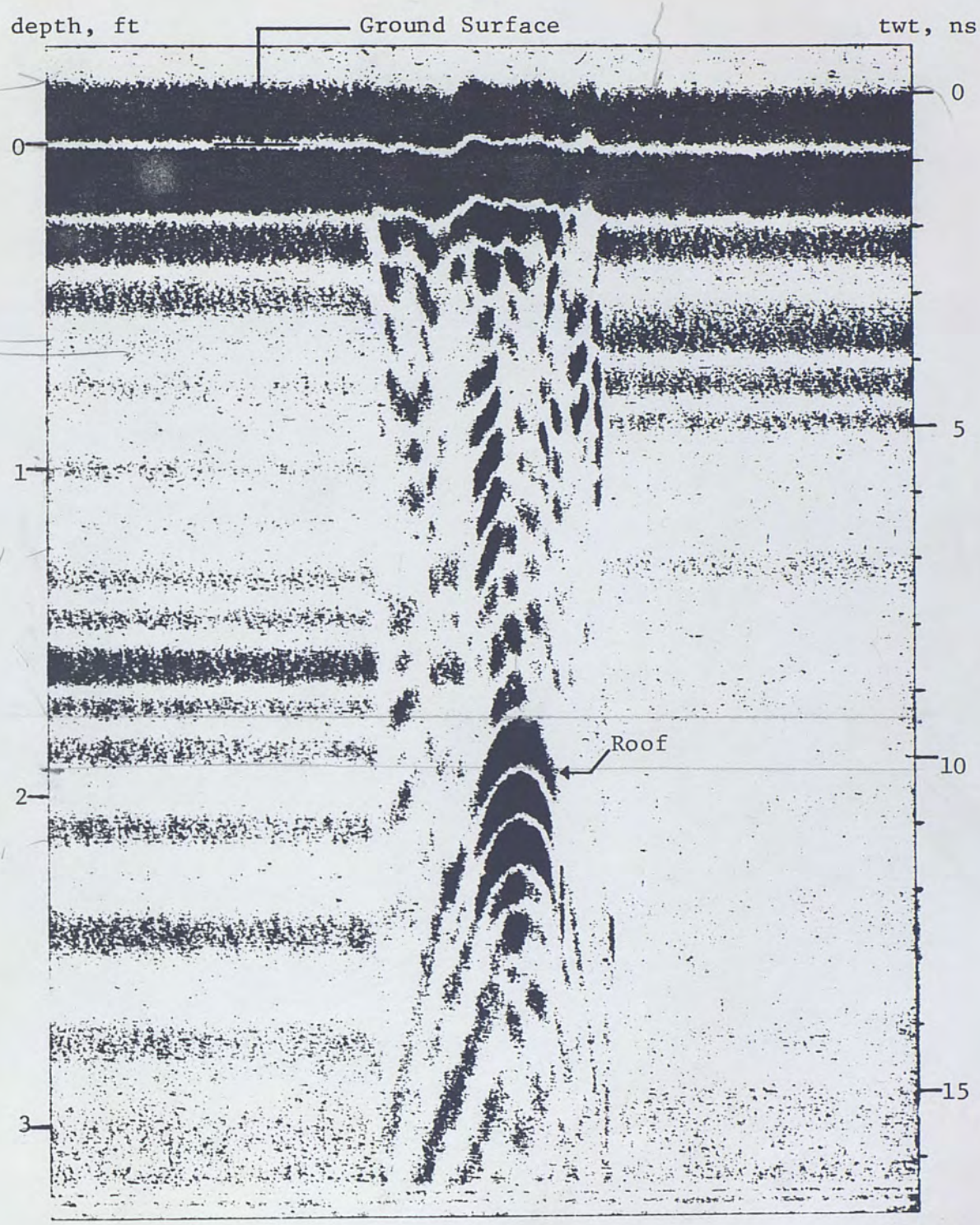

Fig. 9. Profile of cylindrical cavity model, 900 MHz antenna.

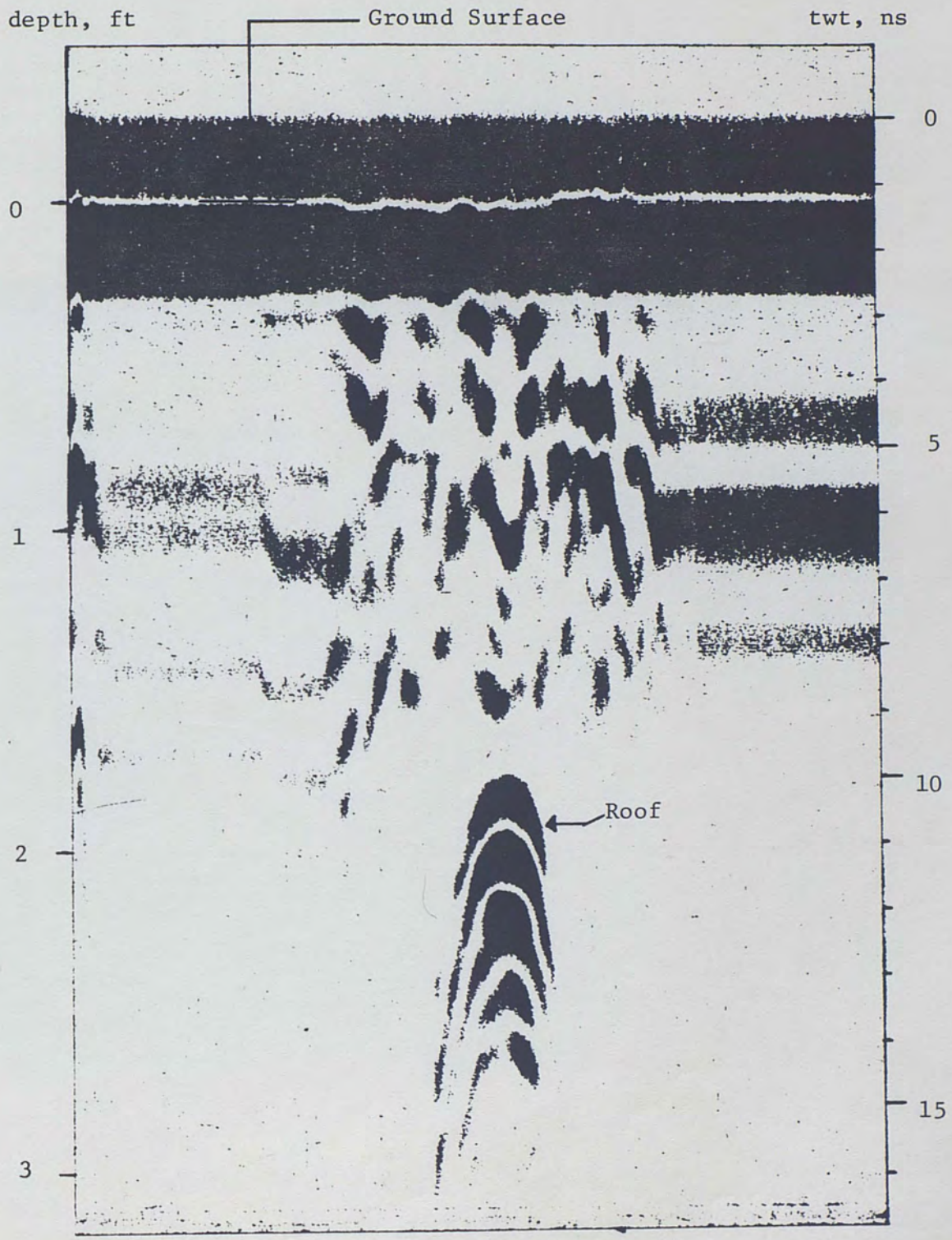

Fig. 10. Profile of cylindrical cavity model, 500 MHz antenna.

corresponds to a normal range adjustment of 0 xl from the calibration chart in the Appendix. The first dark band at the top of the profile is the transmit pulse. The origin of the time scale is located immediately above this band. The dark band below the transmit pulse is the first pulse reflection from the ground surface. The origin of the depth scale (ground surface) is taken as the thin white band created by the crossover in signal polarity between the transmit pulse and this surface reflection as depicted in Figure 9.

The dark bands beneath the surface reflections in Figure 9 are reflections from various subsurface interfaces. The horizontal bands on the left and right sides of the profile are produced when the antenna is stationary. As the antenna begins to move, the subsurface reflections no longer appear horizontal due to irregularities in the soil composition.

The cavity roof is identified by the hyperbolic reflection patterns that appear in the profile of Figure 9. However, the small diameter of the cylinder prevents a clear reflection from the cavity floor. The proximity of the roof and floor interfaces causes oscillations of the cavity roof reflection to almost completely mask the cavity floor reflection.

The known depth of the interface and the two-way pulse travel time of the roof reflection are used to calculate the pulse velocity in the overlying soil. The cavity roof interface is taken as the polarity crossover between the first two hyperbolic reflection

bands as shown in Figure 9. Therefore, a two-way pulse travel time of 9.3 ns between the ground surface reference and the designated cavity roof interface is obtained from the time scale of the profile. By applying equation 3, the pulse velocity is calculated:

$$V = \frac{2R}{twt} = \frac{2(1.9\ ft)}{9.3\ ns} = 0.41\ ft/ns$$

Pulse velocities are traditionally expressed in terms of time per distance for convenience. Therefore, this velocity is expressed as 2.44 ns/ft.

The relative dielectric constant of the overlying material is computed by application of equation 2:

$$\varepsilon_r = \left(\frac{C}{V}\right)^2 = (2.44)^2 = 5.95$$

The computed dielectric constant is in the expected range of 4 to 6 for dry sand as given in Table 1.

This analysis is applied to all of the radar data. The ground surface and subsurface interfaces are consistently identified as polarity crossovers for convenience. This assumption causes the computed velocity to be slightly slower than the actual value, but the error is small and does not significantly affect the accuracy of the results.

Hyperbolic reflection patterns from the cavity roof are also evident in the 500 MHz profile of Figure 10. The resolution of soil interfaces is noticeably poorer in this profile due to the larger signal wavelengths.

The target built for the second test is a 2 foot air-filled cube as shown in Figure 8. This model is constructed with one-quarter inch thick plywood on all sides, and buried at a depth of of 1.75 feet. The radar profiles by the 900 and 500 MHz antennas are shown in Figures 11 and 12, respectively.

The cavity roof interface is identified in Figure 11. Curvature of the cavity roof due to the overburden soil pressure is apparent in this profile. The two-way travel time of 7.9 ns corresponding to the roof interface yields a pulse velocity of 2.26 ns/ft. The computed dielectric constant of the overburden soil is 5.11.

On the 900 MHz profile in Figure 11, three relatively weak horizontal bands below the strong roof reflection appear to be a reflection from the cavity floor. The roof to floor height of the model is 2 feet, therefore the two-way pulse travel distance is 4 feet. Since the pulse velocity in air is 1 ns/ft, the two-way travel time between the roof and floor interfaces should be 4 ns. However, the scaled two-way pulse travel time from the roof interface to the apparent floor interface in Figure 11 is 5.1 ns. This discrepancy is caused by the partial masking of the floor reflection by oscillations of the roof reflection. The computed location of the cavity floor is designated in Figure 11. Note that the floor interface occurs at an apparent depth less than its actual depth of 3.75 ft, because the pulse travels at a much faster velocity in the air-filled cavity than in the surrounding soil.

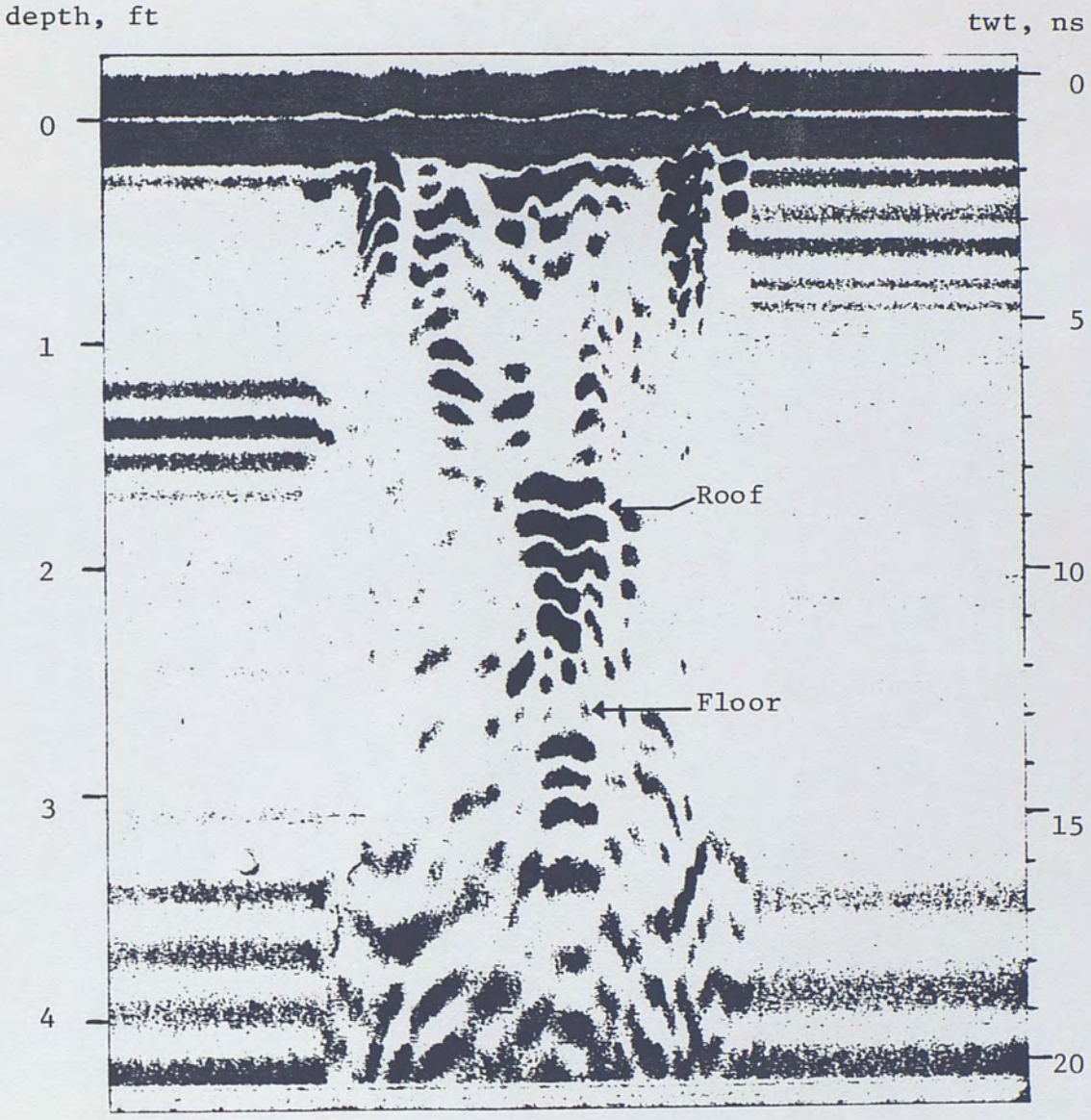

Fig. 11. Profile of cubic cavity model, 900 MHz antenna.

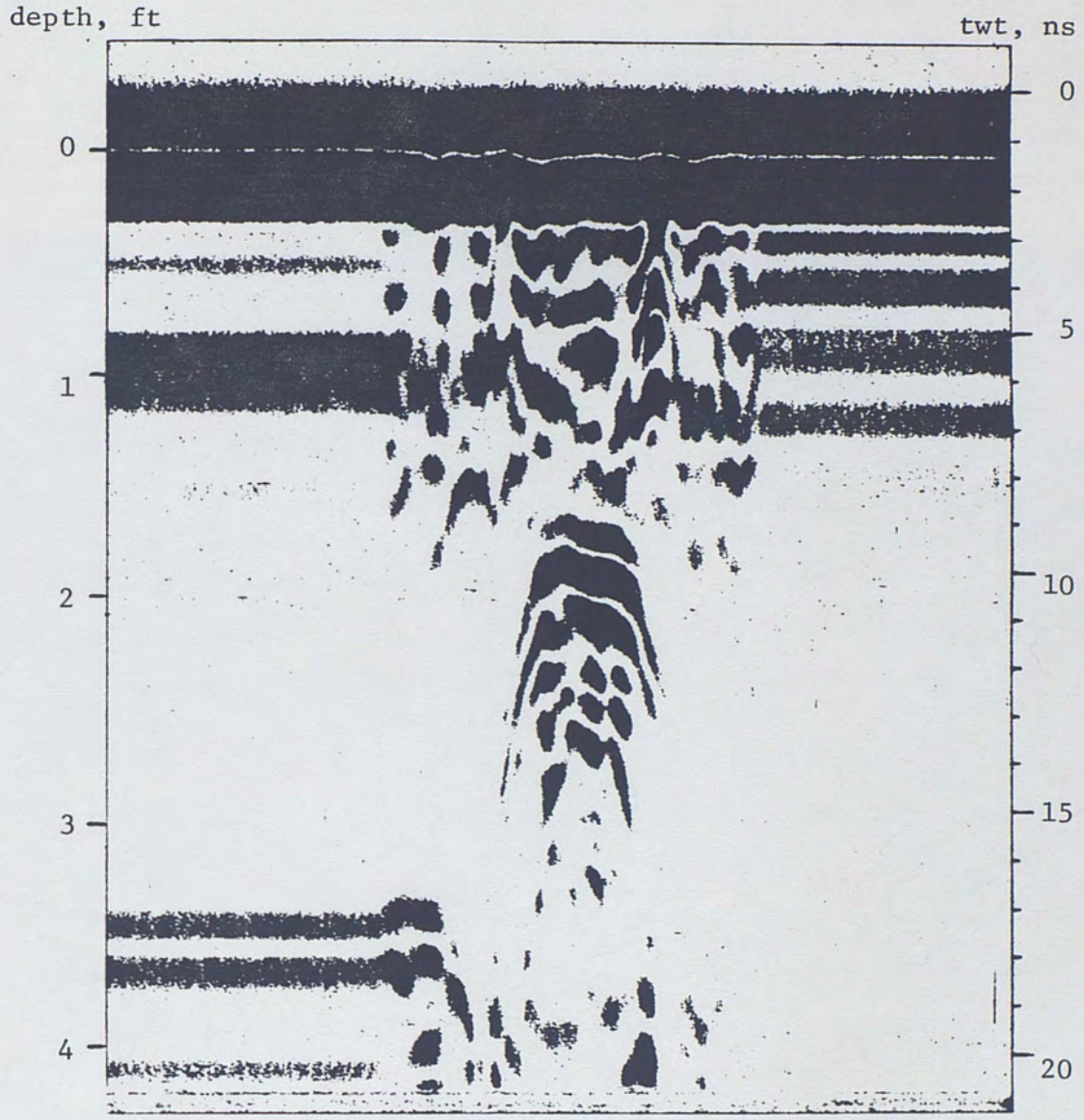

Fig. 12. Profile of cubic cavity model, 500 MHz antenna.

A floor reflection does not appear in the 500 MHz profile of Figure 12, because the larger wavelength signal does not provide sufficient resolution to differentiate the closely spaced roof and floor interfaces.

In the next step of the investigation, two larger and deeper subsurface cavity models were constructed for study. The lining chosen for these models was polyvinyl chloride (PVC) because of its strength, durability and low conductivity which would reduce signal attenuation. A PVC sheet thickness of one-quarter inch was selected as the smallest thickness which could withstand the anticipated soil overburden pressures.

Both cavity models are composed of two identically shaped hemispheres. These hemispheres were formed by heating the PVC sheet and "pushing" or molding it to the desired shape. In the beginning, a spherically shaped void was considered due to the convenience of its circular cross section. However, the process of molding the PVC hemispheres into a spherical shape would severely weaken their strength. To avoid this weakening, the spheres were flattened in the vertical direction to create an ellipsoidal rather than a circular cross section. The PVC cavity models were fabricated by Faulkner Plastics, Inc. of Tampa, Florida.

A diagram of the air-filled PVC cavity is shown in Figure 13. The model is buried at a depth of 2.7 feet from the ground surface to the cavity roof. The horizontal diameter of the cavity is

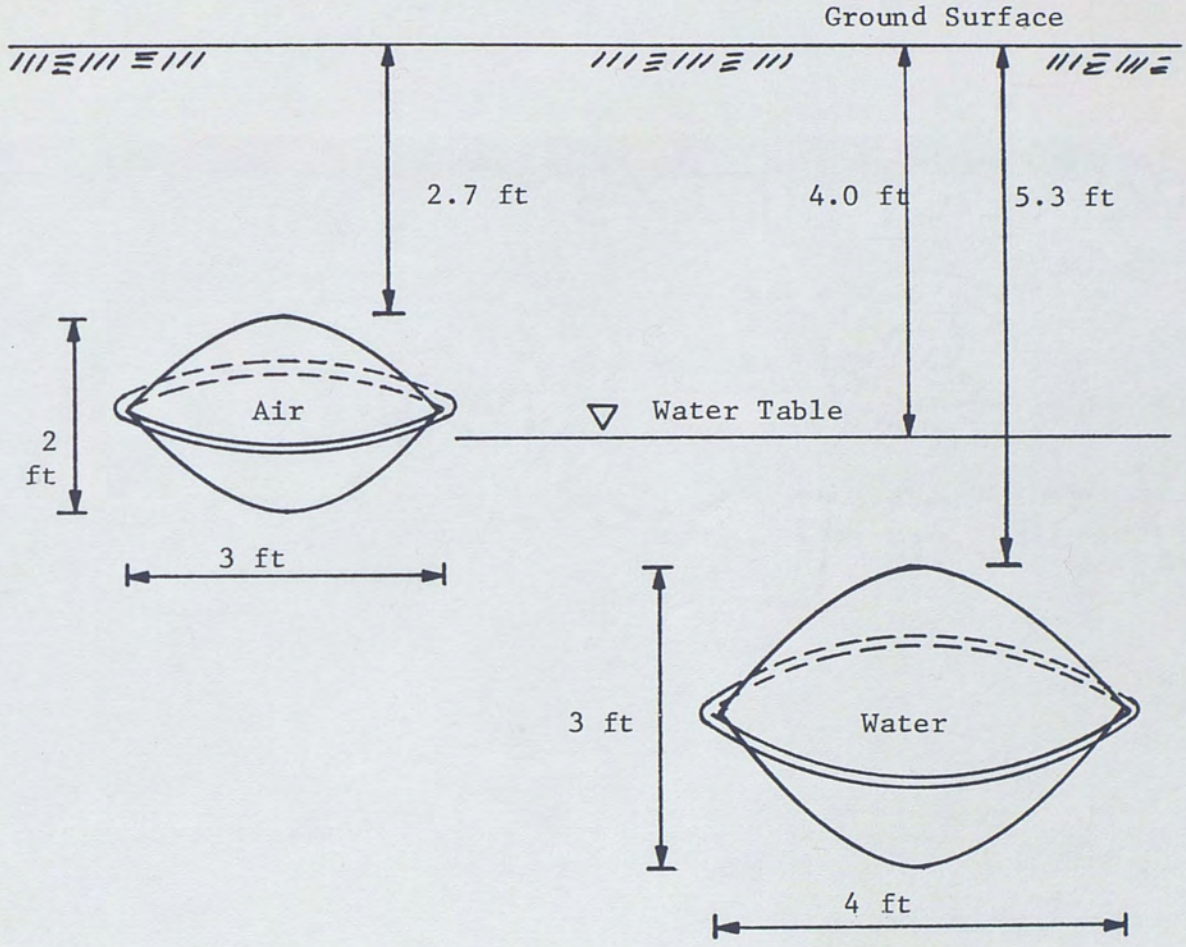

Fig. 13. Air-filled and water-filled PVC cavity models.

3 feet and the maximum distance between roof and floor is 2 feet. Photographs of an excavation for cavity burial and a PVC cavity model are shown in Figures 14 and 15, respectively.

Radar profiles of the air-filled cavity are shown in Figure 16 through 22. These profiles were obtained with radar antenna frequencies of 900, 500, 300, and 80 MHz, respectively. The total scan time, or probing depth, varies among the profiles. A review of these figures reveals a decrease in signal resolution with decreasing frequency. For instance, in the 80 MHz profile of Figure 22, the resolution is so poor that the cavity roof is virtually undetectable. Another consistent pattern among the profiles is the increase in the strength of the cavity reflections with decreasing antenna frequency, due to the smaller signal absorption losses incurred with low frequency antennas. The rapid attenuation of high frequency signals is exemplified in the 900 MHz profile of Figure 16 where the cavity reflections are very weak, indicating that the cavity is located close to the maximum penetration depth of the 900 MHz antenna.

The 900 and 500 MHz profiles shown in Figures 16 and 17, respectively, provide good resolution of near surface features. In these profiles, irregularly shaped random signal reflections appear directly above the cavity. These reflections are the result of the excavation and backfilling of the overburden soil. Soil layers with different electrical properties are blended and numerous random reflections arise from the nonhomogeneous material.

Fig. 14. Excavation at UCF cavity test site.

Fig. 15. PCV cavity model.

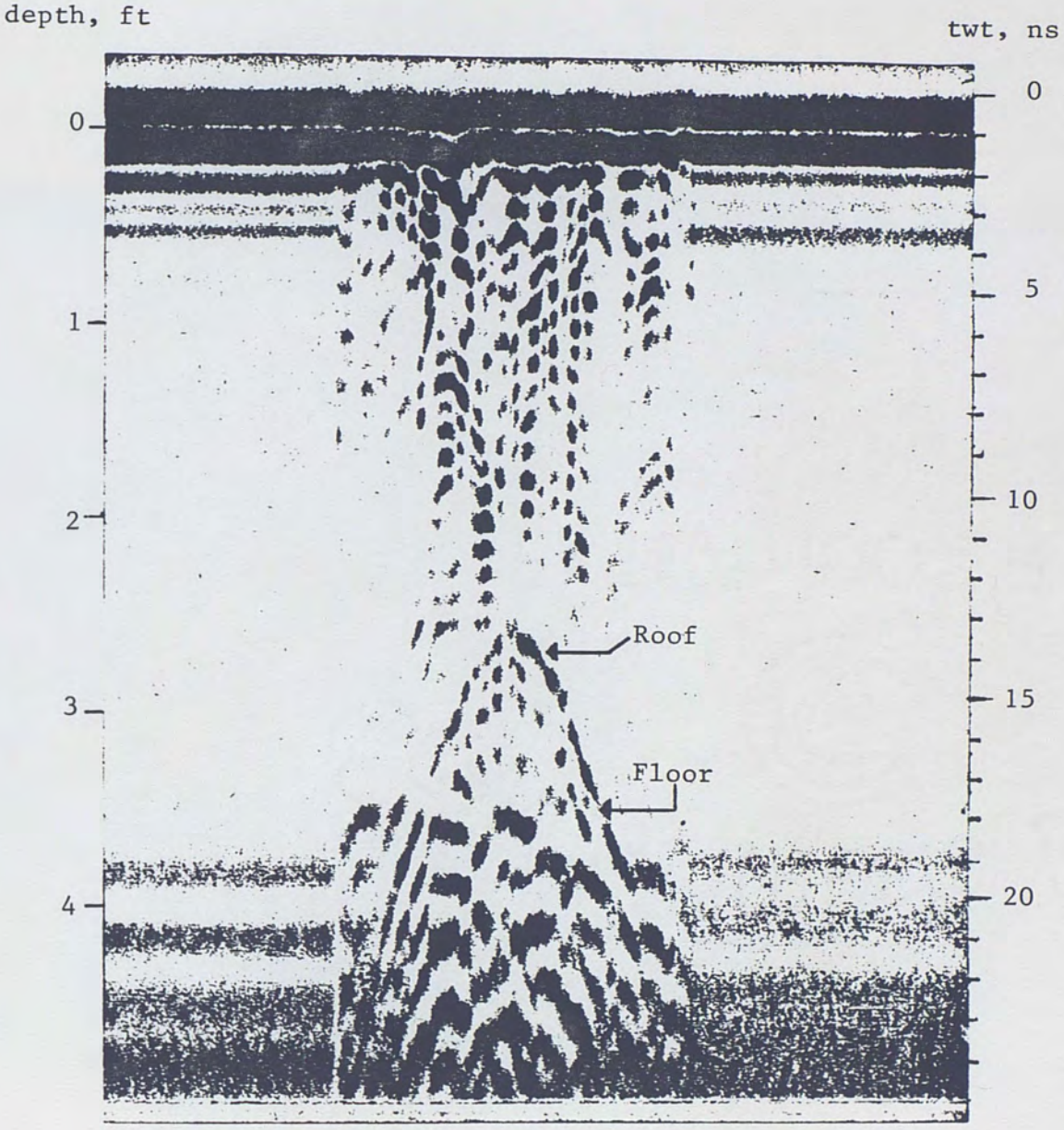

Fig. 16. Profile of PVC air-filled cavity model, 900 MHz antenna.

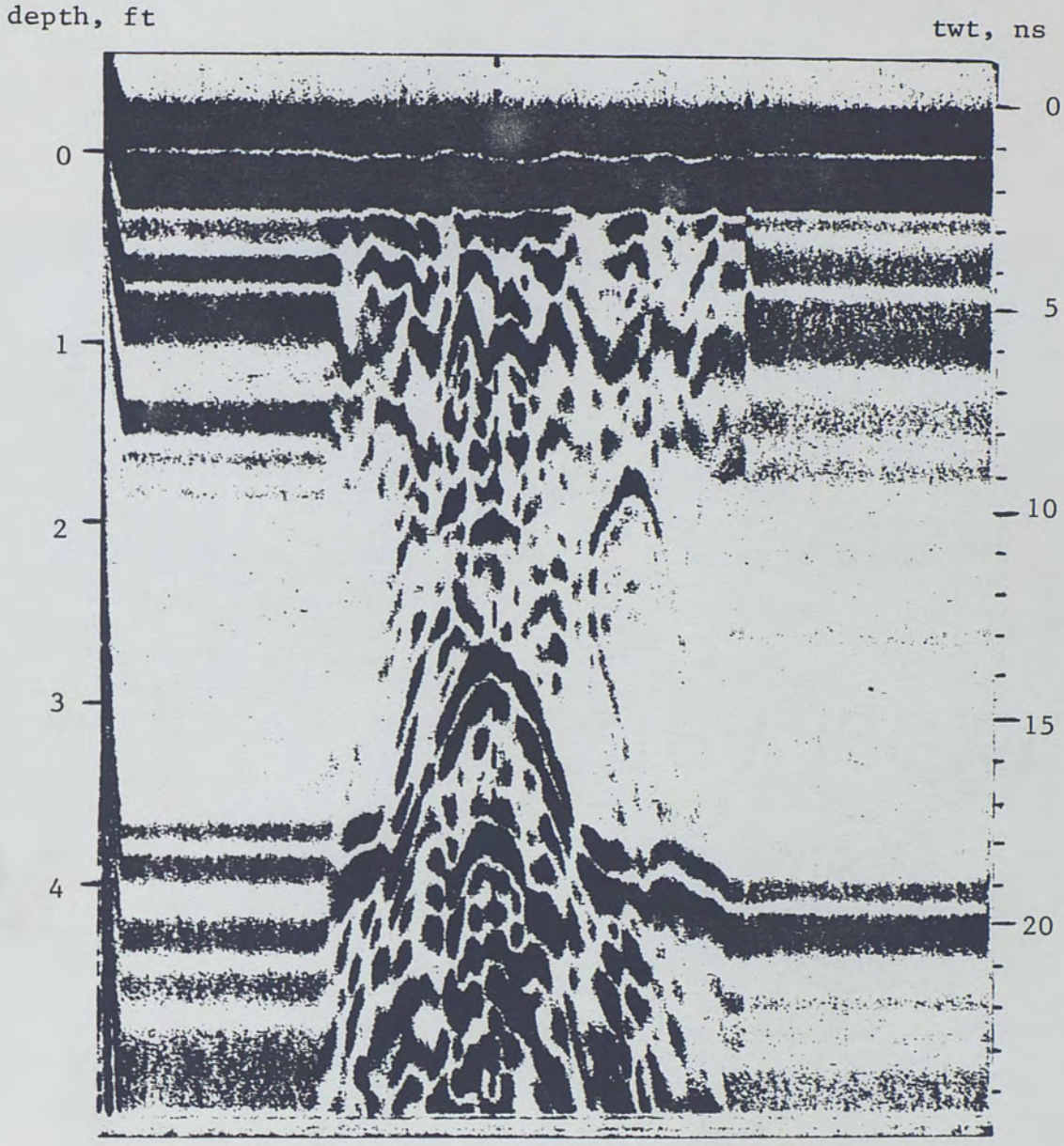

Fig. 17. Profile of PVC air-filled cavity model, 500 MHz antenna, normal range adjustment 200 x 1.

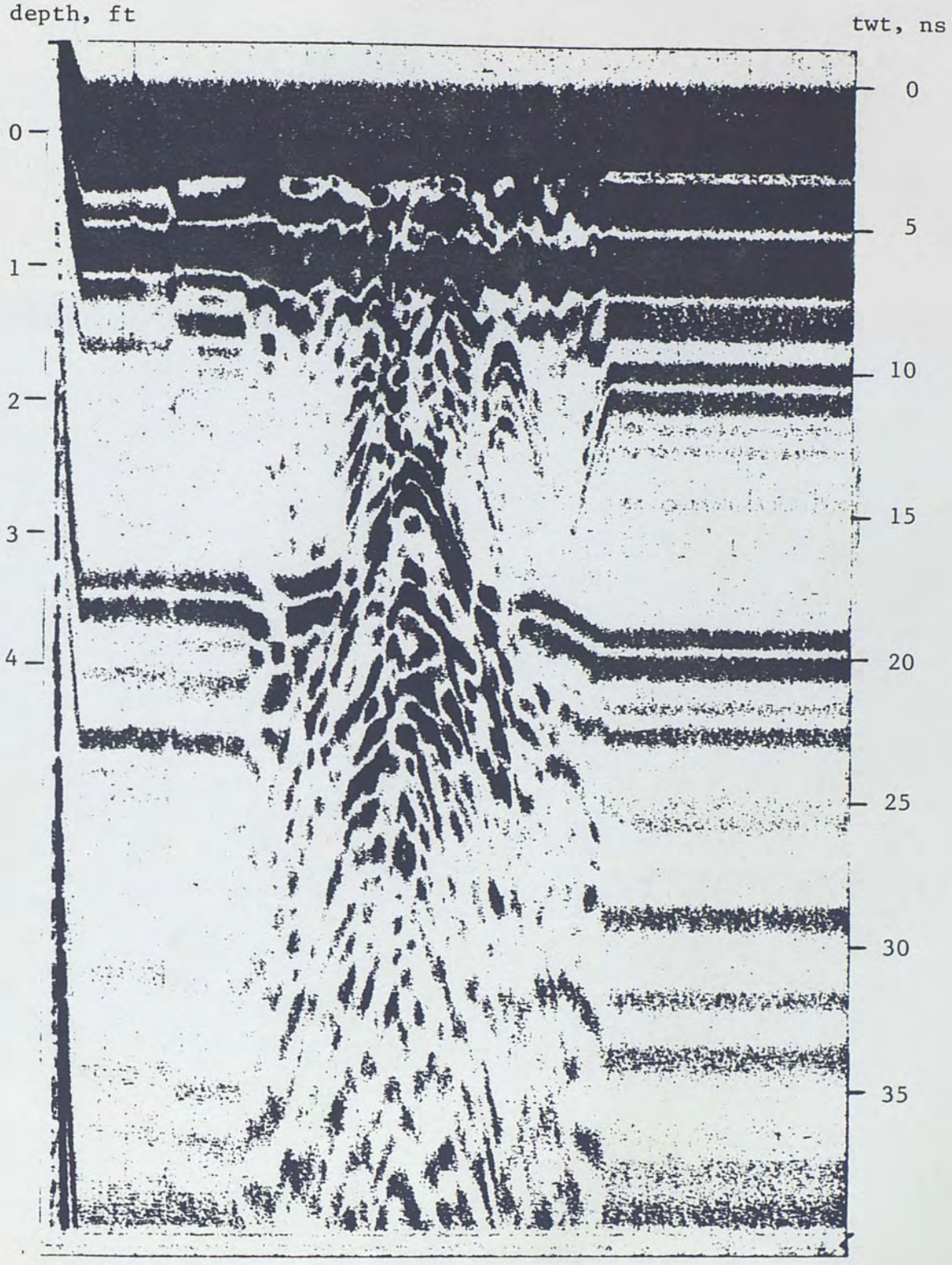

Fig. 18. Profile of PVC air-filled cavity model, 500 MHz antenna, normal range adjustment 100 x 2.

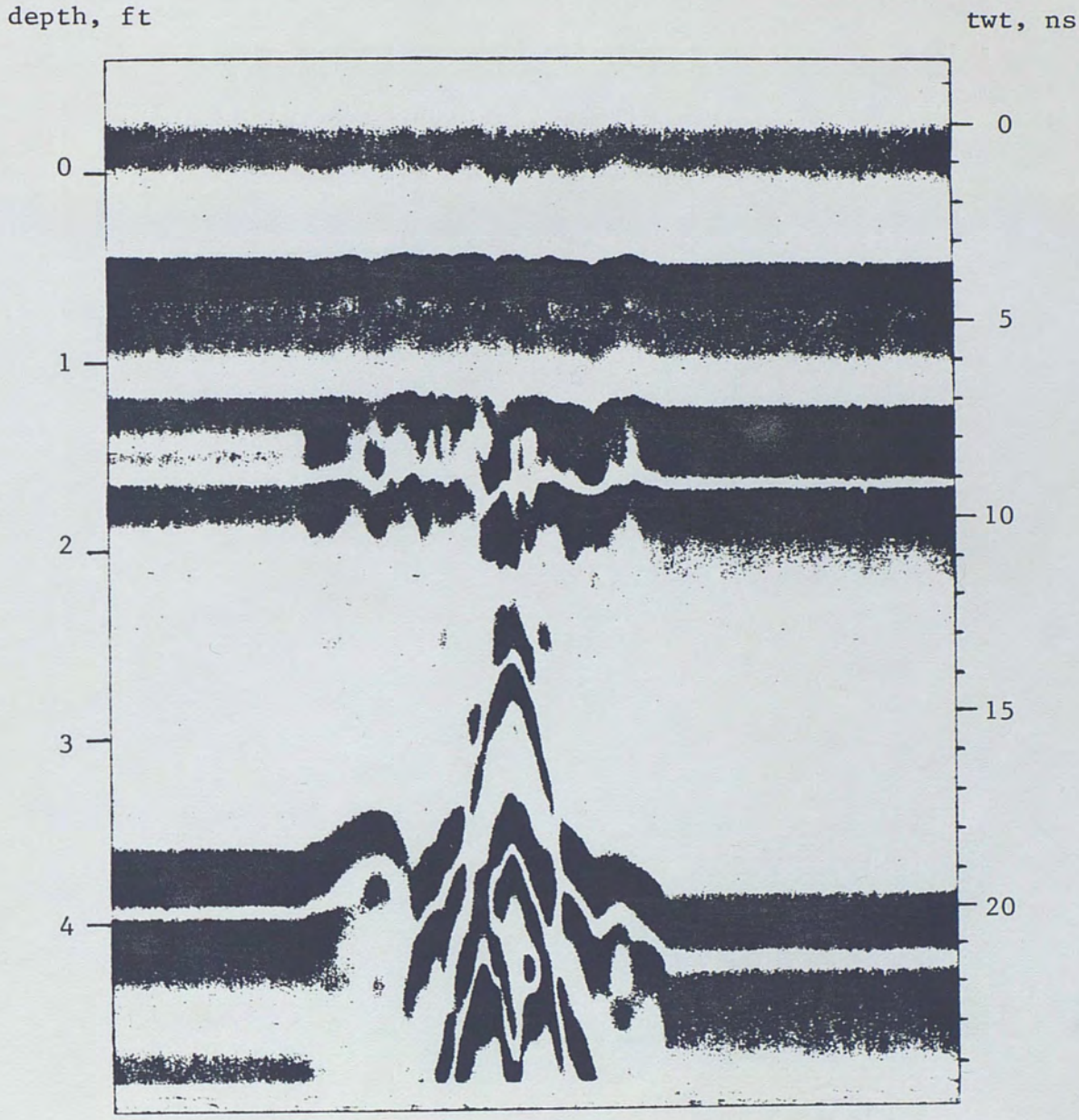

Fig. 19. Profile of PVC air-filled cavity model, 300 MHz antenna, normal range adjustment 200 x 1.

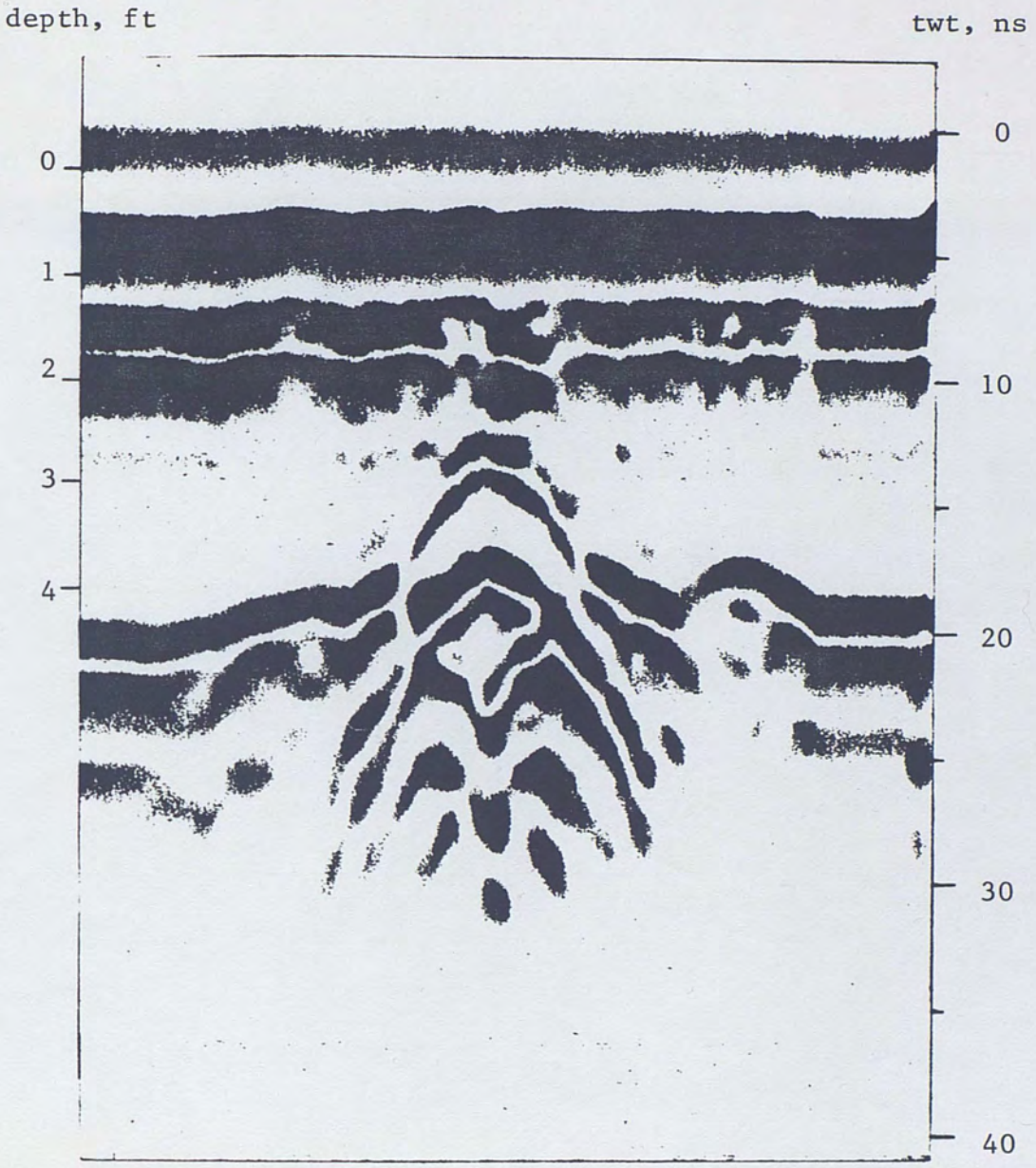

Fig. 20. Profile of PVC air-filled cavity model, 300 MHz antenna, normal range adjustment 100 x 2.

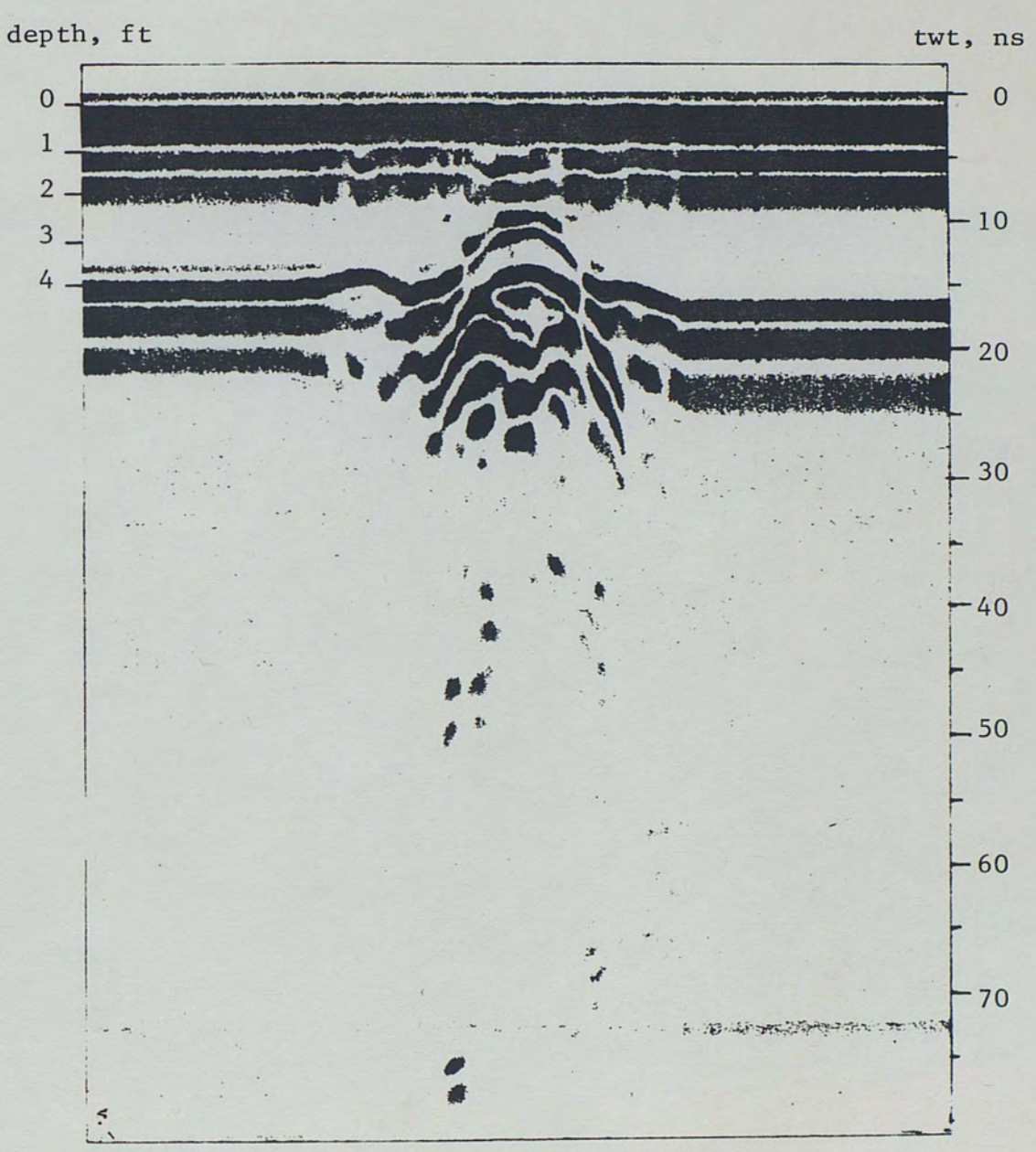

Fig. 21. Profile of air-filled PVC cavity model 300 MHz antenna, normal range adjustment 100 x 4.

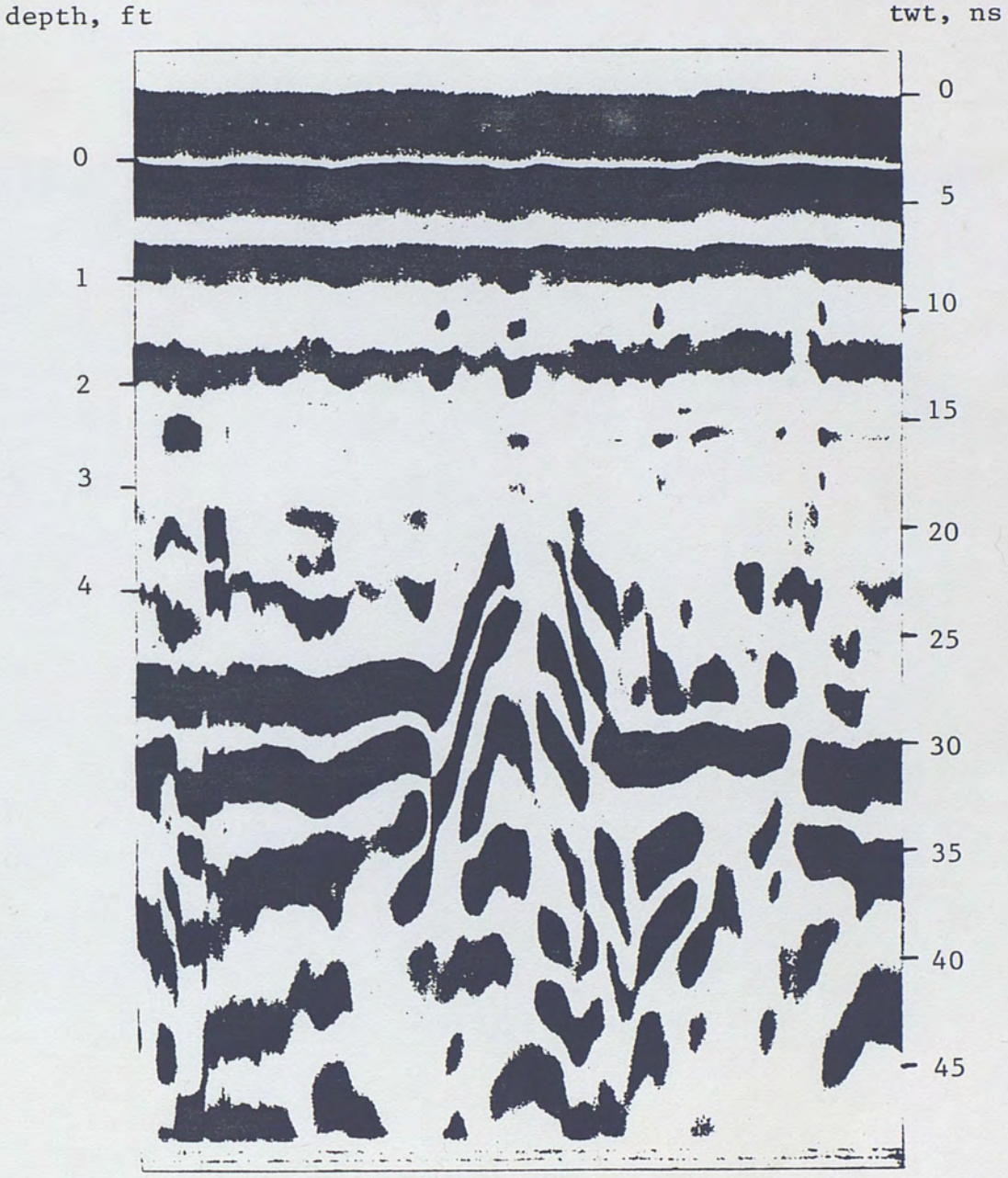

Fig. 22. Profile of PVC air-filled cavity model, 80 MHz antenna.

In Figures 17 through 22, dark bands appear on both sides of the cavity reflection. These bands are a strong reflection from the organic hardpan layer which is common in this part of Central Florida. The hardpan layer is not detected in Figure 16 due to the limited penetration provieed by the 900 MHz antenna.

The reflection from the cavity roof is represented by the dark hyperbolic bands in the radar profiles of Figures 16 through 21. This pattern is expected due to the ellipsoidal cross section of the cavity. A similarly shaped reflection pattern is also expected from the cavity floor, since the shortest signal path to the upwardly concave cavity floor also occurs when the antenna is directly above the center of the cavity. Reflections which appear to emanate from the cavity floor are visible in all the profiles.

In the 900 MHz radar profile of Figure 16, which provides the best resolution of closely spaced interfaces, the apparent cavity floor interface appears about 4.6 ns after the roof interface. However, the actual cavity height of 2 feet should produce a two-way pulse travel time of 4 ns. Oscillations of the roof reflection which partially mask the initial reflection from the floor are responsible for this discrepancy. The PVC cavity lining makes these oscillations more pronounced than they would be under natural cavity conditions. Instead of a single soil-air interface, the lining creates a soil-PVC interface and a PVC-air interface. Oscillations in the reflected pulses from both interfaces are expected. Although the cavity floor is not precisely defined by the radar data, its presence and general

location are evident from segments of its reflection pattern which are not masked. As in the cubic model profile of Figure 11, the reflection from the floor appears at a depth less than the actual floor depth of 4.7 feet due to the faster pulse velocity inside the air-filled cavity.

Another common characteristic of the radar data in Figures 17 through 22 is the presence of multiple reflections from the bottom of the cavity. These reflections are the result of the air-PVC and PVC-soil interfaces at the cavity floor. The transition from excavated soil to natural soil directly beneath the cavity also generates pulse reflections.

Referring to the 900 MHz profile of Figure 16, the two-way pulse travel time from the surface to the cavity roof is 13.2 ns. Since the depth to the cavity roof is known to be 2.7 feet, a pulse velocity of 2.44 ns/ft and a dielectric constant of 5.98 can be calculated for the overburden soil.

Water-filled Cavity

Another PVC cavity model was constructed for burial below the water table. The specifications of this cavity are shown in Figure 13. The excavation had to be pumped dry while the model was put in place. The cavity was filled with water and sealed before it was covered. Its ellipsoidal cross section measures 4 feet horizontally with a maximum vertical height in the center of 3 feet. The cavity roof is 5.3 feet below the ground surface and about 1.3 feet below the water table.

Radar profiles of this cavity using 500, 300 and 80 MHz antennas are shown in Figures 23 through 26, respectively. Due to the rapid attenuation of high frequency signals, the cavity could not be detected with the 900 MHz antenna. Reflections emanating from the cavity are barely visible in the 500 MHz profile (Figure 23), but clear cavity reflections are visible in the 300 MHz profiles (Figures 24 and 25) and the 80 MHz profile (Figure 26).

Referring to the 300 MHz profile of Figure 24, the strong hyperbolic reflection pattern near the bottom of the profile emanates from the cavity floor. The location of the floor interface corresponds to a total two-way travel time of about 95 ns. Floor reflections located at approximately the same two-way time are visible in the 500 MHz profile (Figure 23) and the other 300 MHz profile (Figure 25).

The cavity roof reflection is less apparent than the floor reflection in all of the profiles. In the 500 MHz profile, the roof reflection is completely absent, and only parts of the reflections can be seen in 300 and 80 MHz profiles. Multiple reflections from the nonhomogeneous overburden are responsible for the poor quality of the roof reflection. Because the soil above the cavity was backfilled by earthmoving equipment, a great deal of debris and hardpan became mixed with the overyling sand. These anomolies produce numerous reflections which obscure the cavity roof reflection.

The roof reflection is seen most clearly in the 300 MHz profile of Figure 24. Referring to this figure, the identity of the

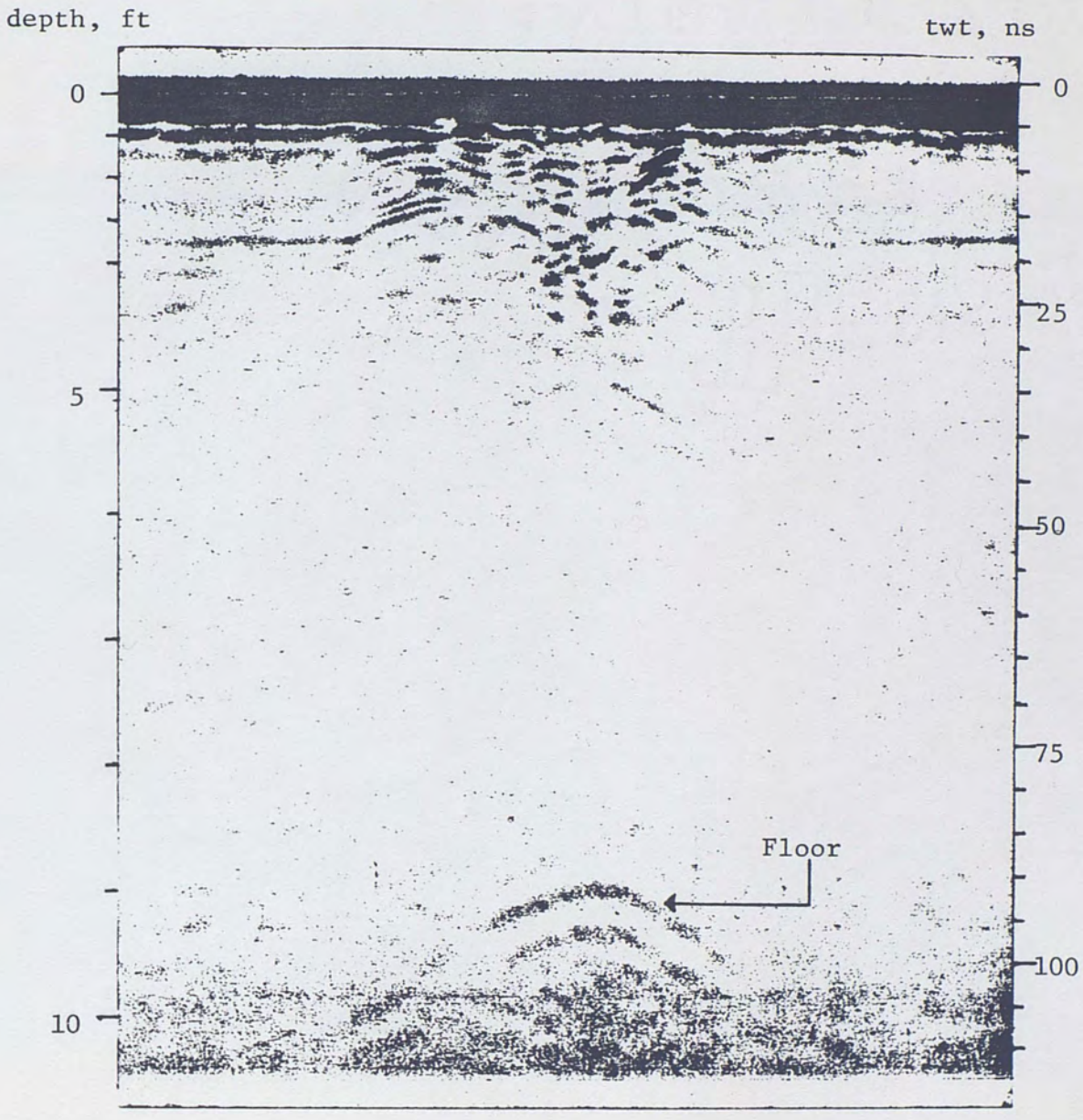

Fig. 23. Profile of PVC water-filled cavity, 500 MHz antenna.

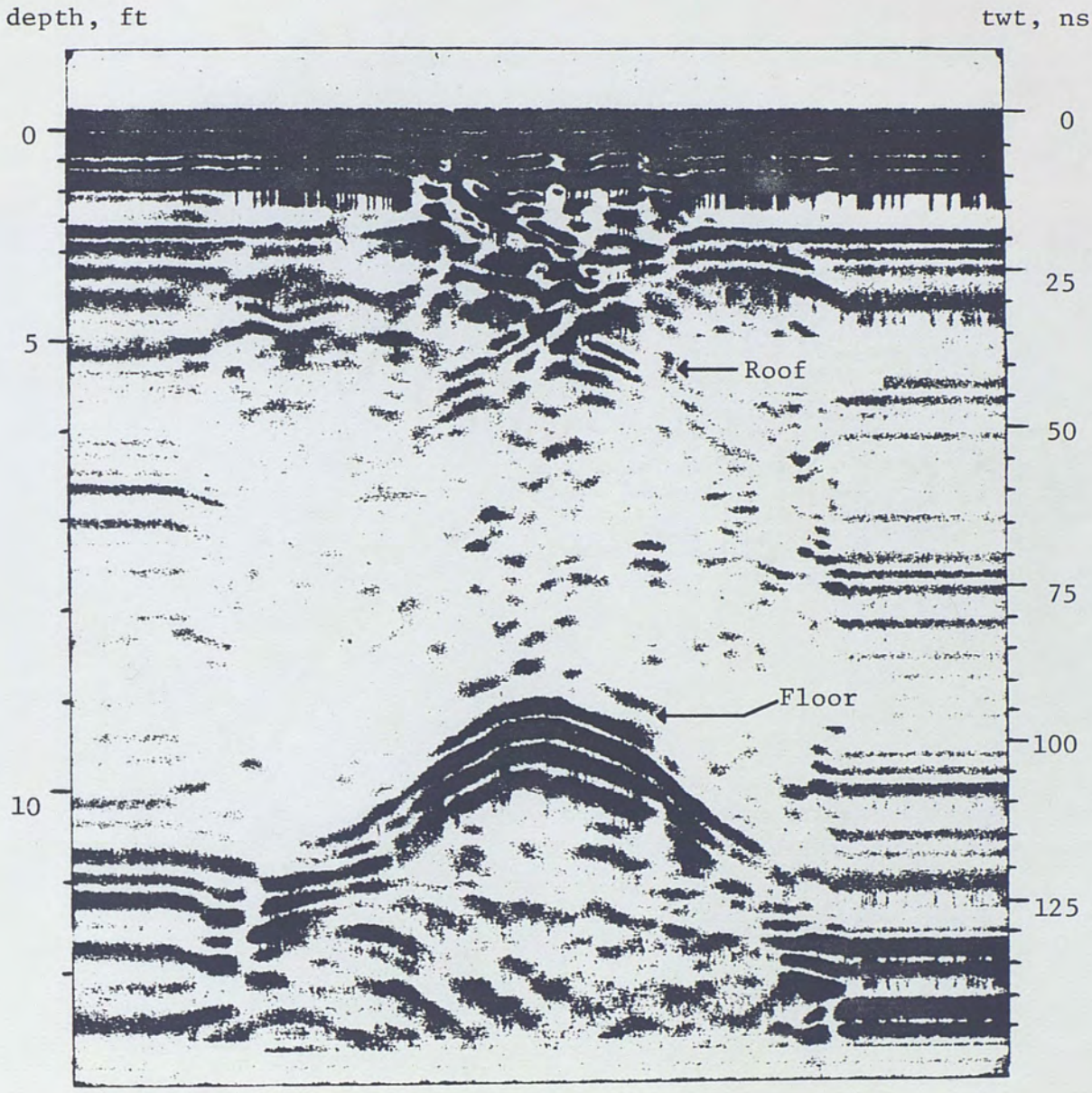

Fig. 24. Profile of PVC water-filled cavity model, 300 MHz antenna, normal range adjustment 500 x 4.

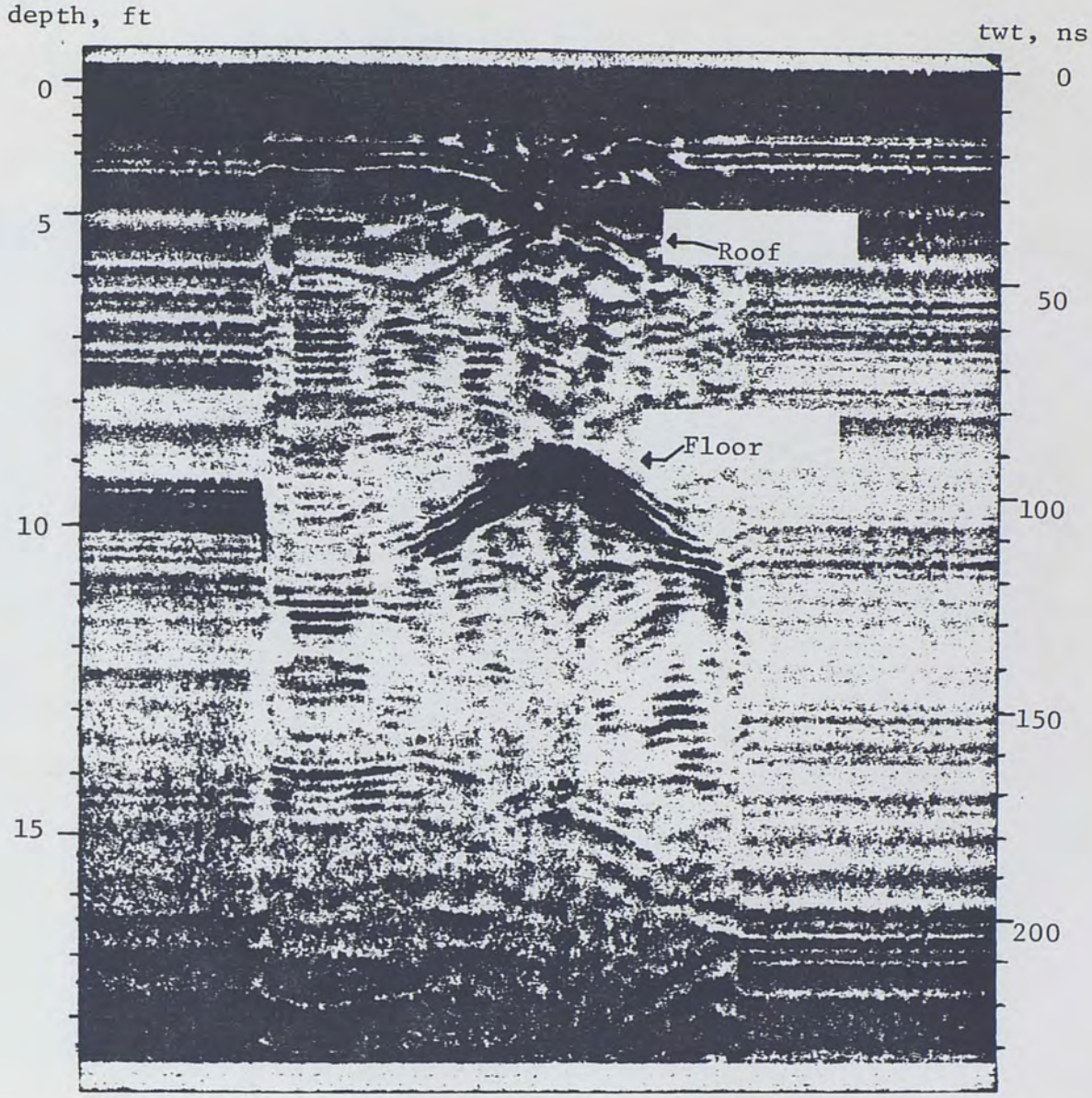

Fig. 25. Profile of PVC water-filled cavity, 300 MHz antenna, normal range adjustment 1000 x 4.

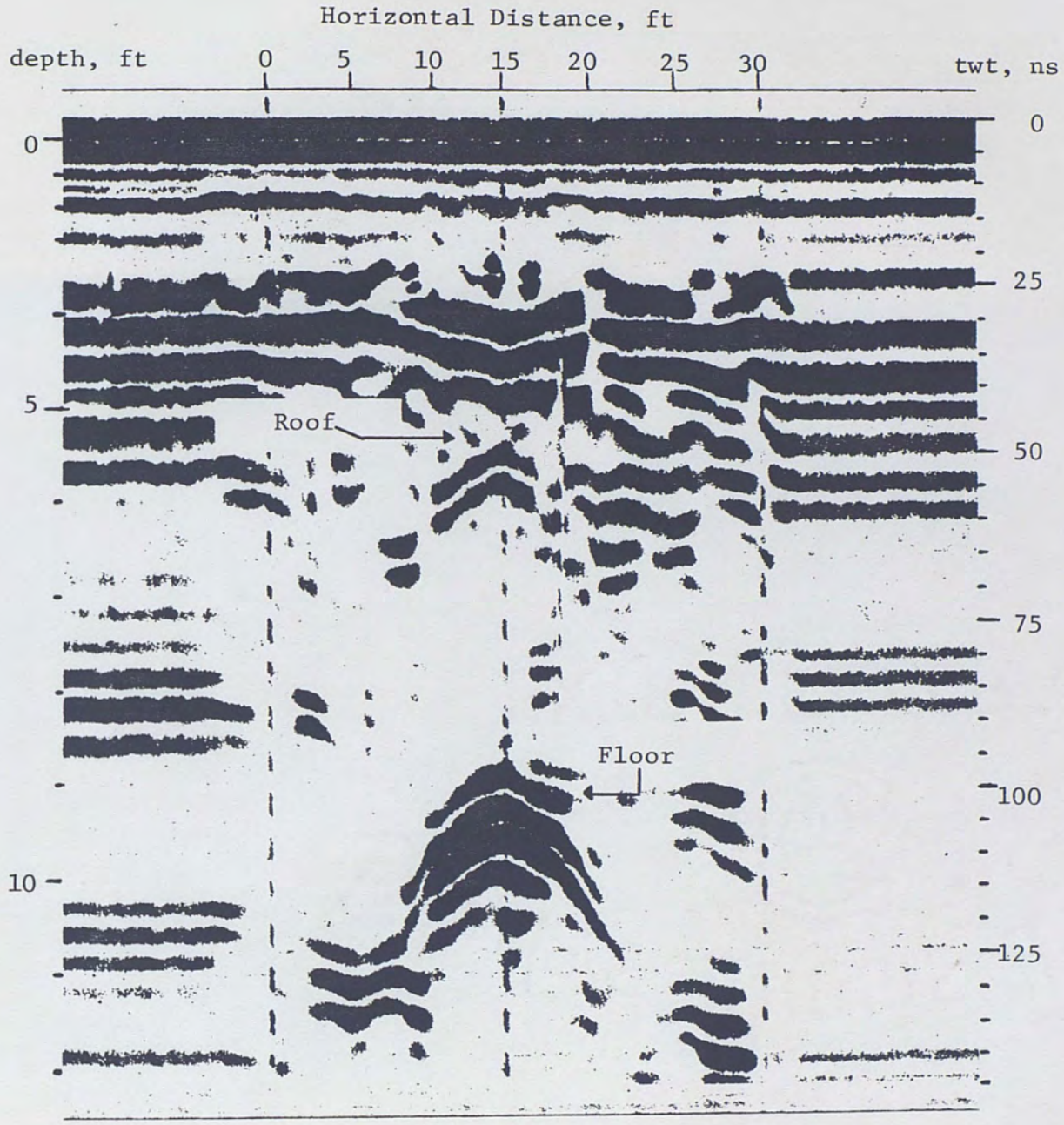

Fig. 26. Profile of PVC water-filled cavity model, 80 MHz antenna.

cavity roof can be verified by computing the difference between the two-way travel times of the roof and floor reflections and comparing this time with the corresponding time measured from the record. The maximum distance between the roof and floor is 3 feet, and the pulse velocity in water is 9 ns/ft. Therefore, a pulse traveling from roof to floor should take 27 ns to make the trip one-way, and the two-way travel time should be 54 ns. The two-way travel time of about 55 ns measured from the record in Figure 24 is sufficiently accurate to verify the identity of the roof and floor reflections.

From Figure 24, the two-way travel time difference between the ground surface interface and the roof interface is approximately 37 ns. An average velocity of 3.5 ns/ft is computed for the soil overburden using the known cavity depth of 5.3 ft. This average pulse velocity is slower than those previously calculated for the soil overlying the cylinder and cube models due to the saturation of the sand below the water table. When Figures 23 through 25 were recorded, the water table was about 4 feet below the ground surface. By assuming a pulse velocity of 2.4 ns/ft for the 4 feet of relatively dry sand above the water table, the velocity in the saturated sand below the water table can be calculated as follows:

$$2(4 \text{ ft})(2.4 \text{ ns/ft}) + 2(1.3 \text{ ft})V = 37 \text{ ns}$$

or,

$$V = 6.8 \text{ ns/ft}$$

In Figure 24, the cavity floor seems to be deeper than its actual depth of 8.3 feet because the depth scale is based on a pulse velocity of 6.8 ns/ft for the saturated sand. The slower pulse velocity of 9 ns/ft in the water-filled cavity causes the floor interface to appear at 9.2 ft.

In Figure 26, the hyperbolic reflection from the cavity floor has a horizontal span of 13 feet, but, as shown in Figure 13, the water-filled cavity has a horizontal span of four feet. The radar reflection pattern is more than 3 times larger than the actual cavity in this direction due to the formation of a hyperbolic reflection pattern from a curved surface as illustrated in Figure 7.

In the 80 MHz profile of Figure 26, the floor reflection appears at a two-way travel time of 102 ns. The first reflection from the roof is not visible on the record, but because the two-way pulse travel time between the roof and floor is 54 ns, the roof reflection should appear at 48 ns. The increase in these two-way travel times over the times recorded in the other profiles is due to an increase in the moisture content of the sand above the cavity. The data in Figure 26 was taken after a period of heavy rain, which increased the water content in the soil above the cavity and lowered the average pulse velocity to 4.2 ns/ft.

CHAPTER V

GPR FIELD INVESTIGATION

Profiling in Limestone

To gain an insight into the performance of Ground Penetrating Radar under actual field conditions, several radar surveys were conducted in the Gainesville, Florida area. Due to the existing geologic conditions of soluble limestone underlying an unconsolidated overburden, subsurface cavities and sinkholes are common in the central part of the state. Figure 27 is an example of the radar data obtained during this investigation.

A soil profile with a maximum depth of 20 feet was available for the area where the radar data was obtained. The soil overlying the limestone is classified as poorly graded, fine sand. The exact depth of the water table was not shown in the profile, but is known to be deeper than 20 feet. Based on Table 1, an average dielectric constant constant of 8, corresponding to a pulse velocity of 2.8 ns/ft, is estimated for both the sand and limestone material. By applying this velocity, the total two-way scan time of 286 ns is equivalent to a probing depth of about 50 feet. An 80 MHz antenna was used in this survey to achieve the maximum signal penetration.

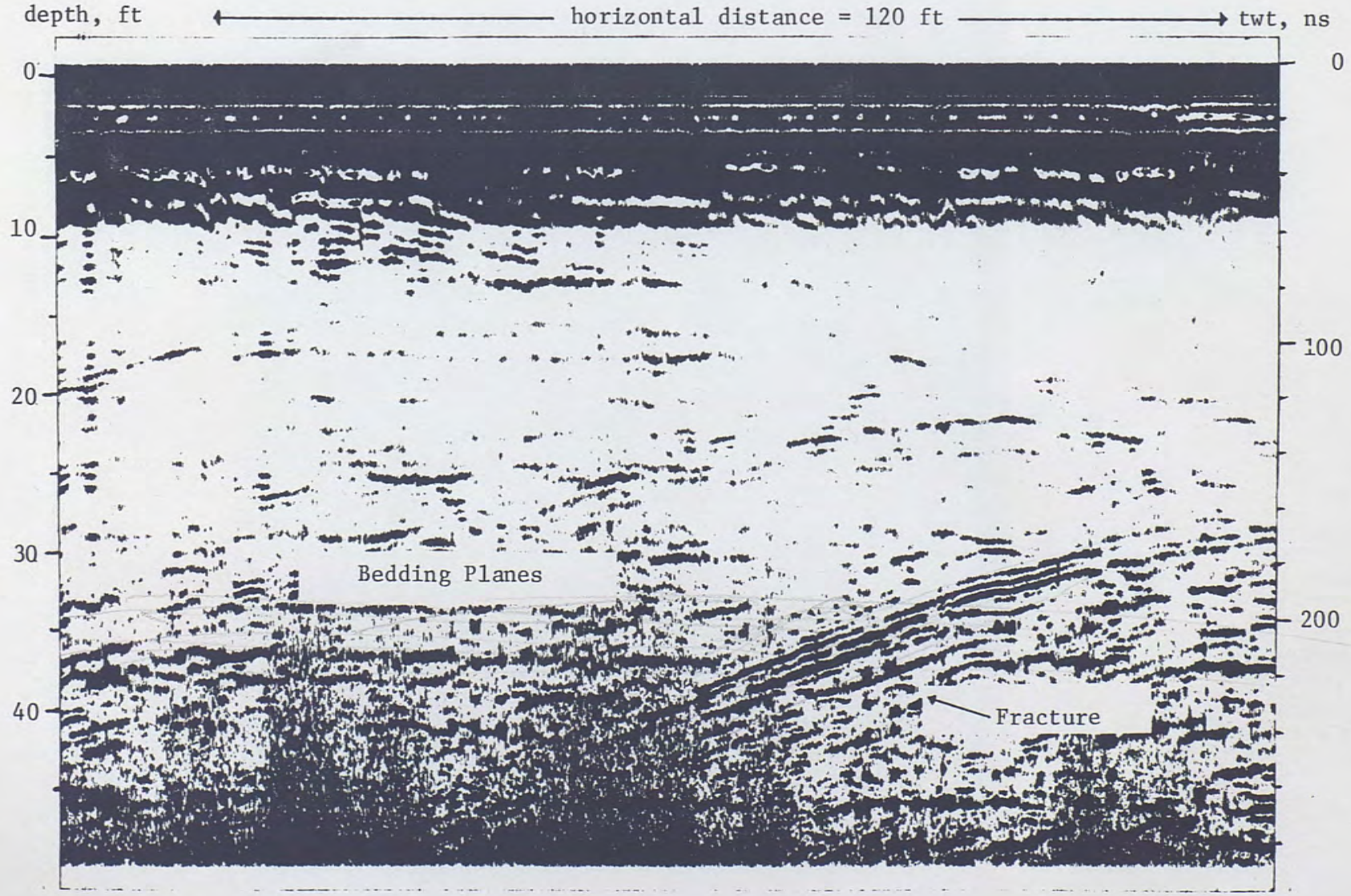

Fig. 27. Radar profile in limestone.

In Figure 27, horizontal bedding planes in the limestone are evident at depths of 30 feet or greater. The essentially blank areas below the strong surface reflection is believed to be relatively homogeneous sand. As shown in the figure, the bedding planes are disrupted by a fracture plane extending from 30 to 40 feet deep.

The profile of Figure 27 is an example of GPR performance under very favorable subsurface conditions. The fairly dry sandy overburden and the underlying limestone are both relatively transparent to radar signals because the low conductivity of these materials keeps signal attenuation to a minimum. Although the subsurface conditions in this profile are favorable, the grainy black areas near the bottom of the profile are representative of a low signal-to-noise ratio. The presence of this noise indicates that the radar signal is close to its maximum penetration depth.

Other radar surveys conducted in the same general area were limited to penetration depths of 10 to 20 feet. The presence of thick clay layers at these sites rapidly attenuated the radar signal and limited penetration. This rapid attenuation was due to the relatively high conductivity of clay as shown in Table 1. In areas with slight amounts of clay in the subsurface profile, maximum penetration depths of 40 to 50 feet were possible.

Subsurface Cavity Profile

A GPR investigation was conducted in the Gainesville area to locate subsurface cavities. The Fort Clarke-Deerhaven power

transmission line was being constructed over a region prone to subsurface cavity and sinkhole formation. Subsurface information was needed at some sixty transmission pole sites to locate any subsurface cavities which might possibly threaten the pole foundations.

Figure 28 is a radar profile obtained during this investigation. An average dielectric constant of 8 is used to estimate the pulse velocity in the subsurface materials consisting of alternate layers of sand, clayey sand, and sandy clay. The water table is believed to be lower than the radar profile depth. Using this information, the total two-way scan time of 175 ns corresponds to a probing depth of 30 feet. The large hyperbolic reflection on the right side of the profile is believed to emanate from a subsurface cavity at a depth of 9-10 feet. The horizontal extent of the reflection pattern is about 60 feet, indicating a possible cavity diameter of 15 to 20 feet, based on the expansion factor observed during the cavity modeling study.

The vertical dashed line to the left of the hyperbolic reflection is the proposed location of the transmission pole. Immediately to the left of the pole position is a zone of disturbance characterized by closely spaced, roughly hyperbolic reflections. This zone is interpreted as a cavity area containing deposits of loose sand or clay material which gives rise to the numerous reflections. As a result of this subsurface information, the pole was relocated to a position 80 feet north of the previous site.

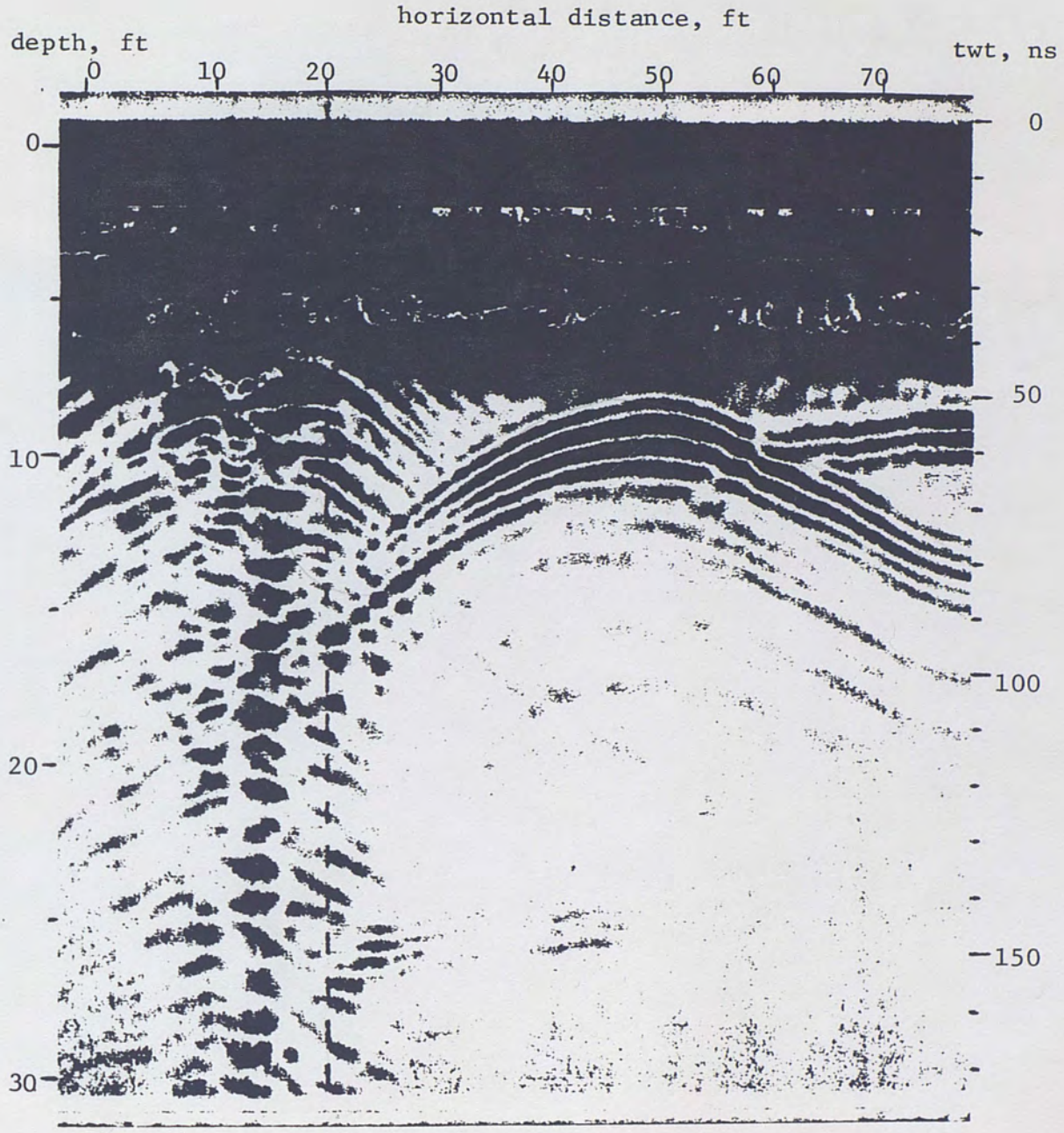

Fig. 28. Cavity zone near proposed transmission pole site in Gainesville, Florida.

Lake Profile

As previously stated, many lakes in the Central Florida area were created by sinkhole formation. The ability of radar signals to penetrate water makes it possible to profile lake bottoms. Figure 29 is a profile of Lake Claire, located on the campus of the University of Central Florida.

The data was obtained by placing an 80 MHz antenna in an inflatable raft and towing the raft beside a power boat. The radar equipment was operated from the boat, and several transects were made to obtain the cross section which cuts through the center of the depressions.

The total two-way scan time of the profile is 412 ns. The depth scale in Figure 29 is calculated by taking the dielectric constant of the water equal to 81, which corresponds to a pulse velocity of 9 ns/ft. The pulse velocity in the underlying lake bottom and sediment deposits is unknown. From the radar profile of Figure 29, the greatest water depth is about 11 feet. This value was confirmed by actual depth measurements.

The lake appears to have formed from two large sinkhole depressions. The steep sides of the lake descend rapidly toward the throats of the former sinkholes. The relatively weak signals overlying the two deep depressions emanate from the surface of thick organic muck deposits. The firm sandy lake bottom is characterized by a strong signal reflection.

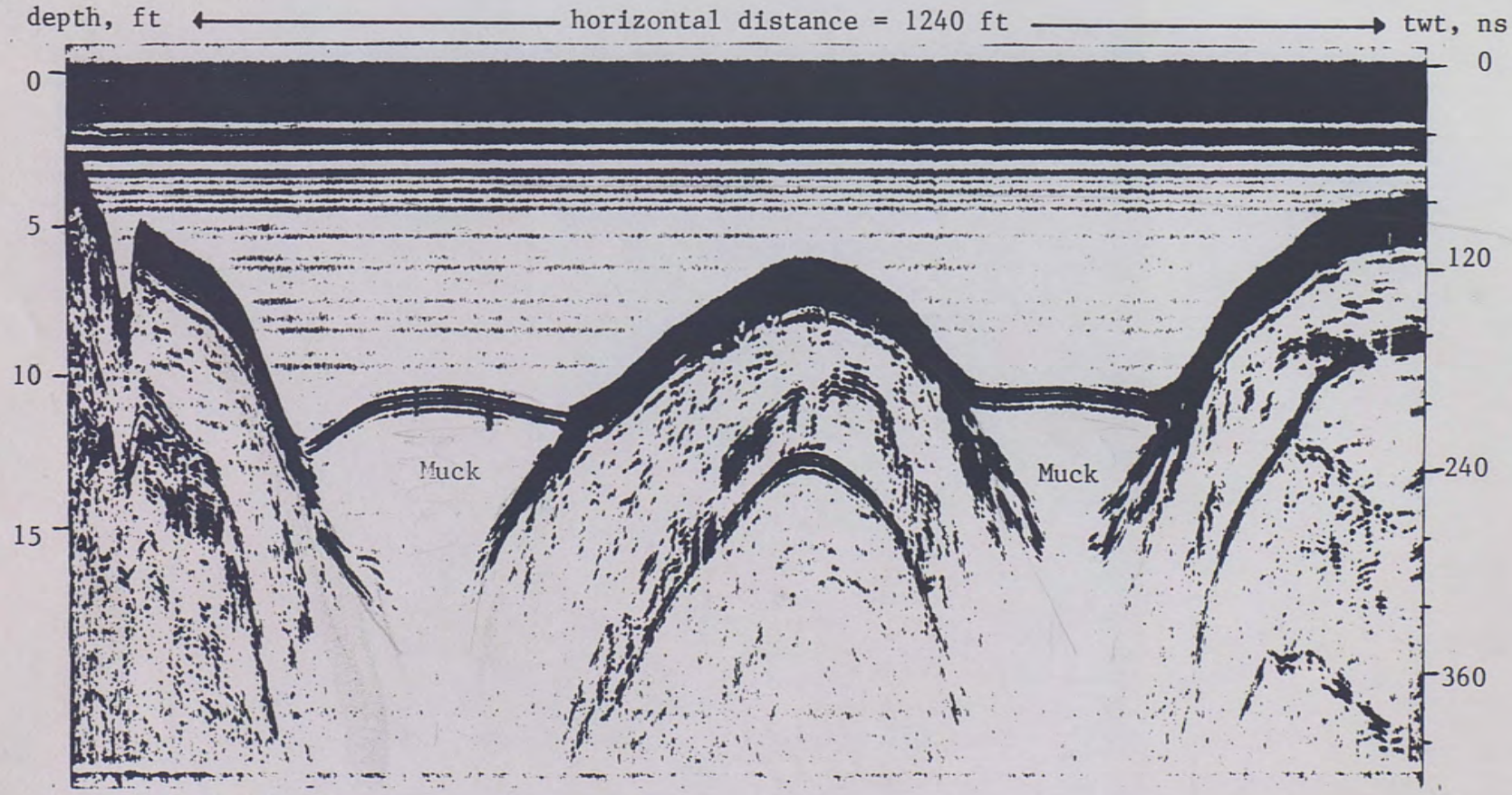

Fig. 29. Lake Claire radar profile.

An interesting feature of the profile is the double reflection from the lake bottom. This "echo" is caused by the entrapment of the radar signal between two highly reflective interfaces. Initially, the radar signal penetrates the water surface and travels through the water until it is reflected from the lake bottom back to the antenna. However, some of the signal energy is reflected from the water surface before reaching the antenna. This energy is again reflected from the lake bottom and received by the antenna, thus creating the double reflection.

Despite the complication of the second reflection from the bottom, several subsurface interfaces can be identified below the lake bottom. A continuous layer is evident in the center of the lake between the two depressions. This interface is located above the second bottom reflection and follows the general contours of the bottom terrain.

CHAPTER VI

SUMMARY AND CONCLUSIONS

Ground Penetrating Radar identifies subsurface features by distinguishing materials with different dielectric constants and electrical conductivities. The radar signal is transmitted into the ground by an antenna and is reflected back to the same antenna by various interfaces between different subsurface materials. The delay time of the reflected signal is then recorded by the radar system. By studying a continuous pattern of reflected signals versus delay time, subsurface features can be delineated. The depth to an interface can be determined if the pulse velocity in the material is known. Subsurface cavities can therefore be detected by the variation in their electrical properties from the electrical properties of the surrounding material.

Subsurface cavity models of varying size, shape, depth and content were profiled by the GPR system. The cavity models were created by excavating to the desired depth, emplacing a lining, and backfilling with the excavated soil. Three air-filled cavity models were placed above the water table, and one water-filled model was located beneath the water table. Strong reflected signals were received from the roofs of the air-filled models. Radar signals reflected from the floor of the two larger air-filled cavities were

also identified, but were partially masked by oscillations of the roof reflection. Radar profiles of the water-filled cavity model showed strong reflections from the floor rather than the roof. In this case, the roof reflection was partially masked by reflections emanating from disturbances in the backfilled overburden.

The reflections from the cavity models with circular or ellipsoidal cross sections formed a hyperbolic pattern. This hyperbolic signature is due to the reflective characteristics of curved interfaces. The cubic cavity model was characterized by horizontal reflections from both roof and floor.

The hyperbolic pattern formed by reflections from an ellipsoidal cavity interface was found to be about 3 times larger than the actual model size in the horizontal direction.

In this study, the groundwater table was found to have a significant effect on the interpretation of the radar data. At the cavity test site, when the transmitted pulse reached the water table, its velocity decreased to about one-third of its velocity above the water table. This velocity decrease caused an elongation of the depth scale on the graphical record.

Radar signal frequency was also found to have a significant effect on the cavity detection ability of GPR. The higher frequency antennas provided better resolution of cavity features than the low frequency antennas. However, high frequency signals were attenuated rapidly, thereby limiting the penetration depth of the radar probe. For the soil conditions and water table depth at the cavity test

site, the 900 and the 500 MHz antennas were limited to penetration depths of approximately 4 and 9 feet, respectively.

The low frequency 300 and 80 MHz antennas allowed deeper signal penetration than the two higher frequency antennas used in the study. However, the larger wavelength signal transmitted by these antennas provided poorer resolution of closely spaced interfaces. This poor resolution makes features near the surface particularly difficult to distinguish due to large oscillations of the surface reflection. The selection of antenna frequency is critical and should be based on the electrical properties of the subsurface material, the depth of interest and the size of the subsurface target.

During the field investigation, the best results were obtained with the 80 MHz antenna in areas of sandy soil overlying limestone. Penetration depths of 40 to 50 feet in these areas made it possible to map limestone features such as bedding planes and fractures. However, in areas with significant clay content in the subsurface medium, signal penetration was limited to 10 to 20 feet due to the relatively high conductivity of clay which causes rapid attenuation of the radar signal. Based on knowledge gained from the cavity modeling study, a subsurface cavity was identified during a GPR investigation near Gainesville, Florida.

The radar system provided excellent information on the subsurface features of Lake Claire. A continuous profile of the lake bottom was obtained from which the water depths could be accurately

determined. The location and size of muck deposits in the sinkhole depressions could also be easily distinguished. The radar record continued to provide information past the lake bottom into the underlying soil.

From the results of this investigation, it is concluded that GPR is an effective cavity detection technique, but only under subsurface conditions which are favorable to the propagation of radar signals.

A great deal remains to be learned about the effect of various subsurface conditions on signal propagation. Accurate assessment of the pulse velocity is essential for interpretation of the radar data. Research is needed to classify pulse velocities for the wide array of soils to be found in the Central Florida area. Knowledge of the effect of soil stratification and water content on pulse velocity is also essential for proper data interpretation. The attenuation rate of the radar signal in various subsurface mediums is another topic which requires thorough investigation.

Ground Penetrating Radar shows great promise as a subsurface exploration technique. Improvements in radar equipment design and the development of interpretive skills will make GPA even more effective in the near future.

APPENDIX

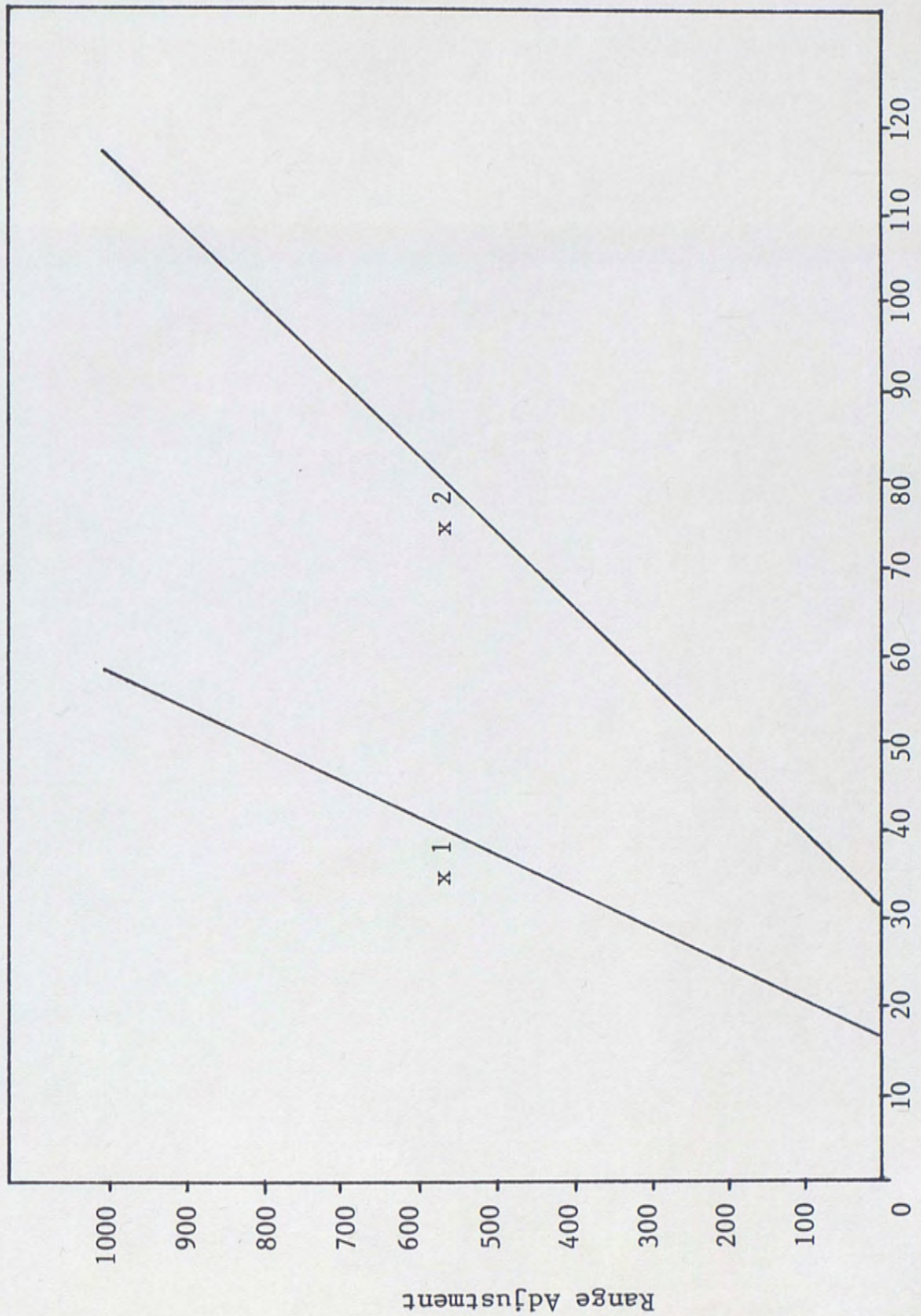

Fig. 30. Normal range calibration chart.

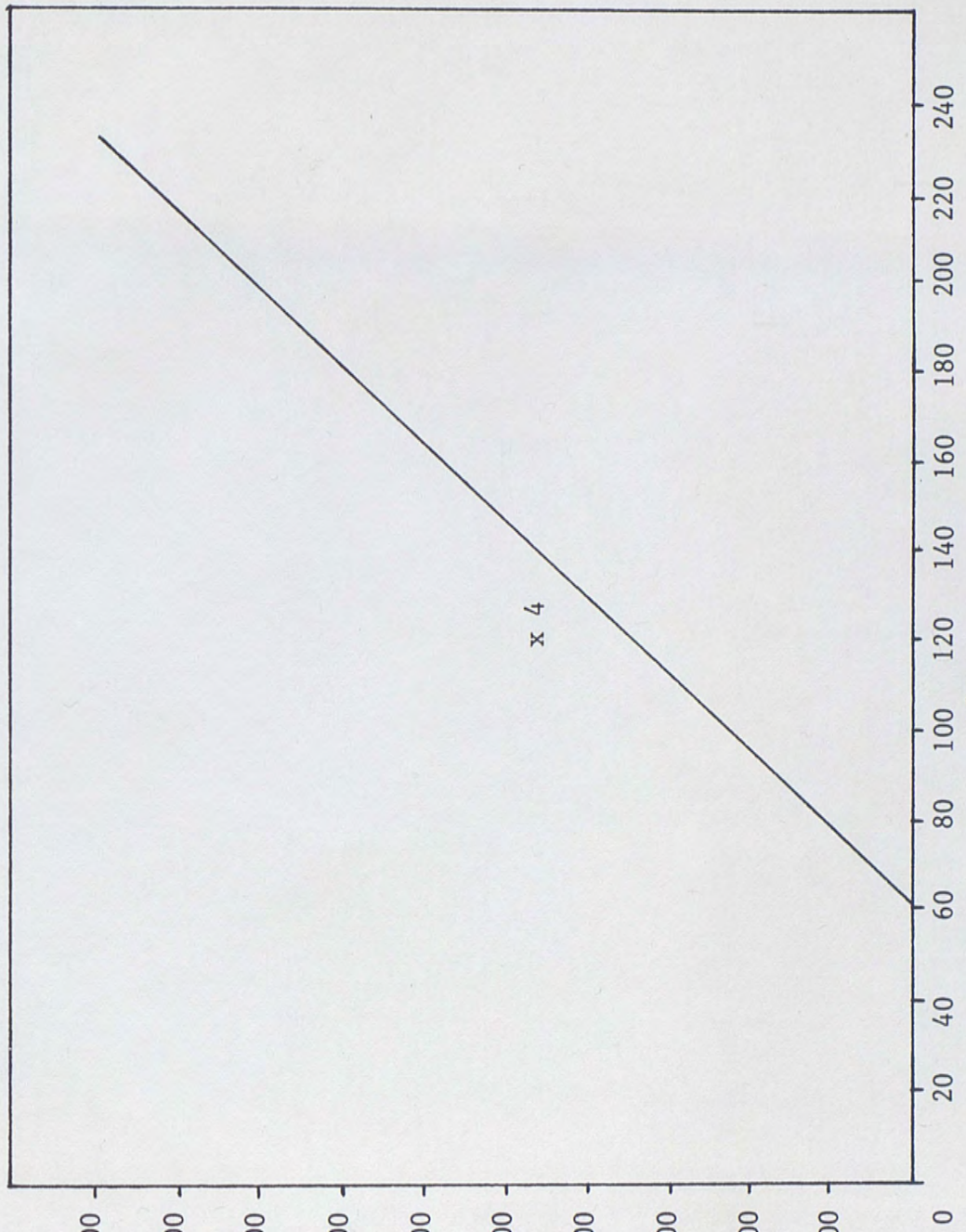

Fig. 31. Normal range calibration chart.

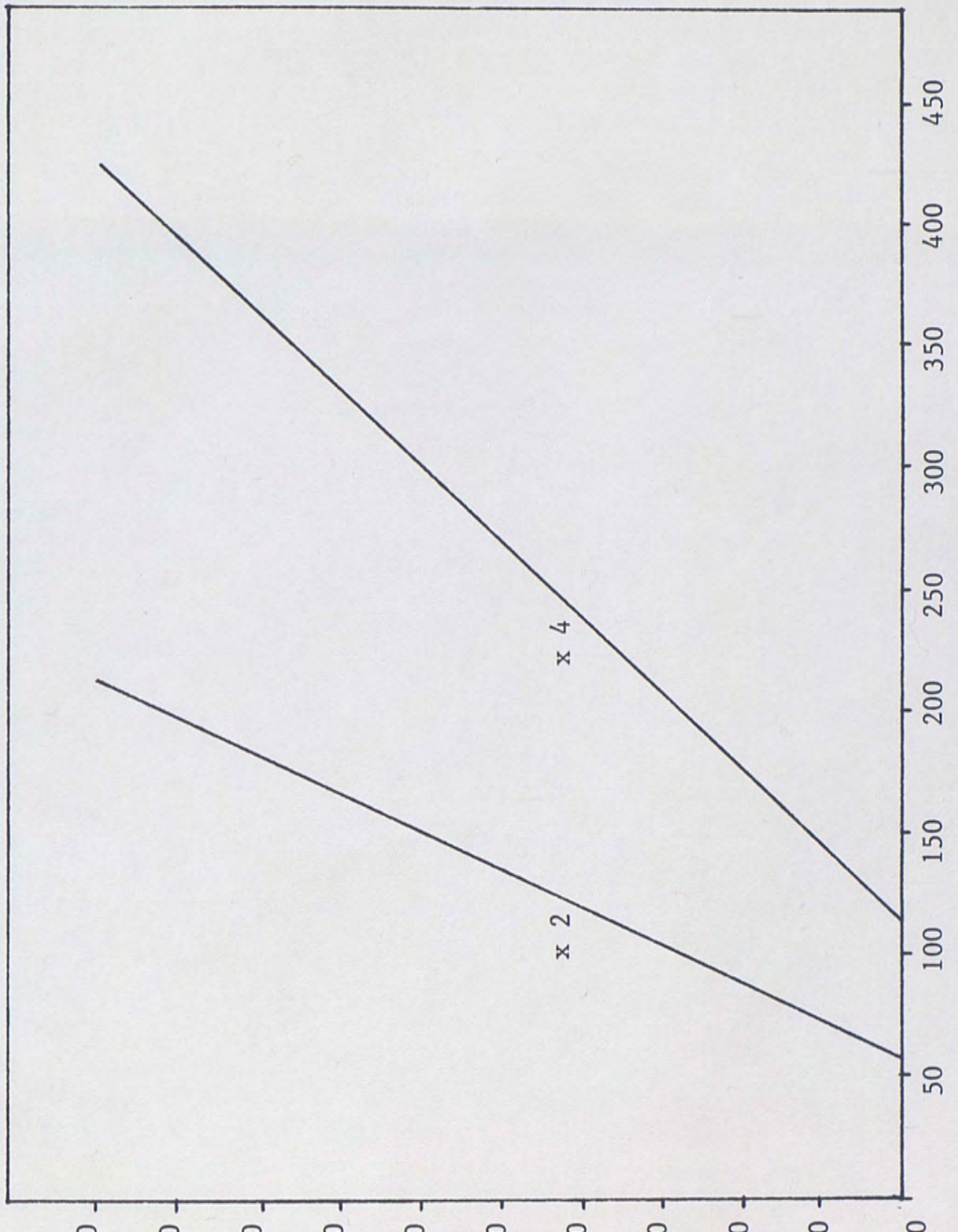

Fig. 32. Ultimate range calibration chart.

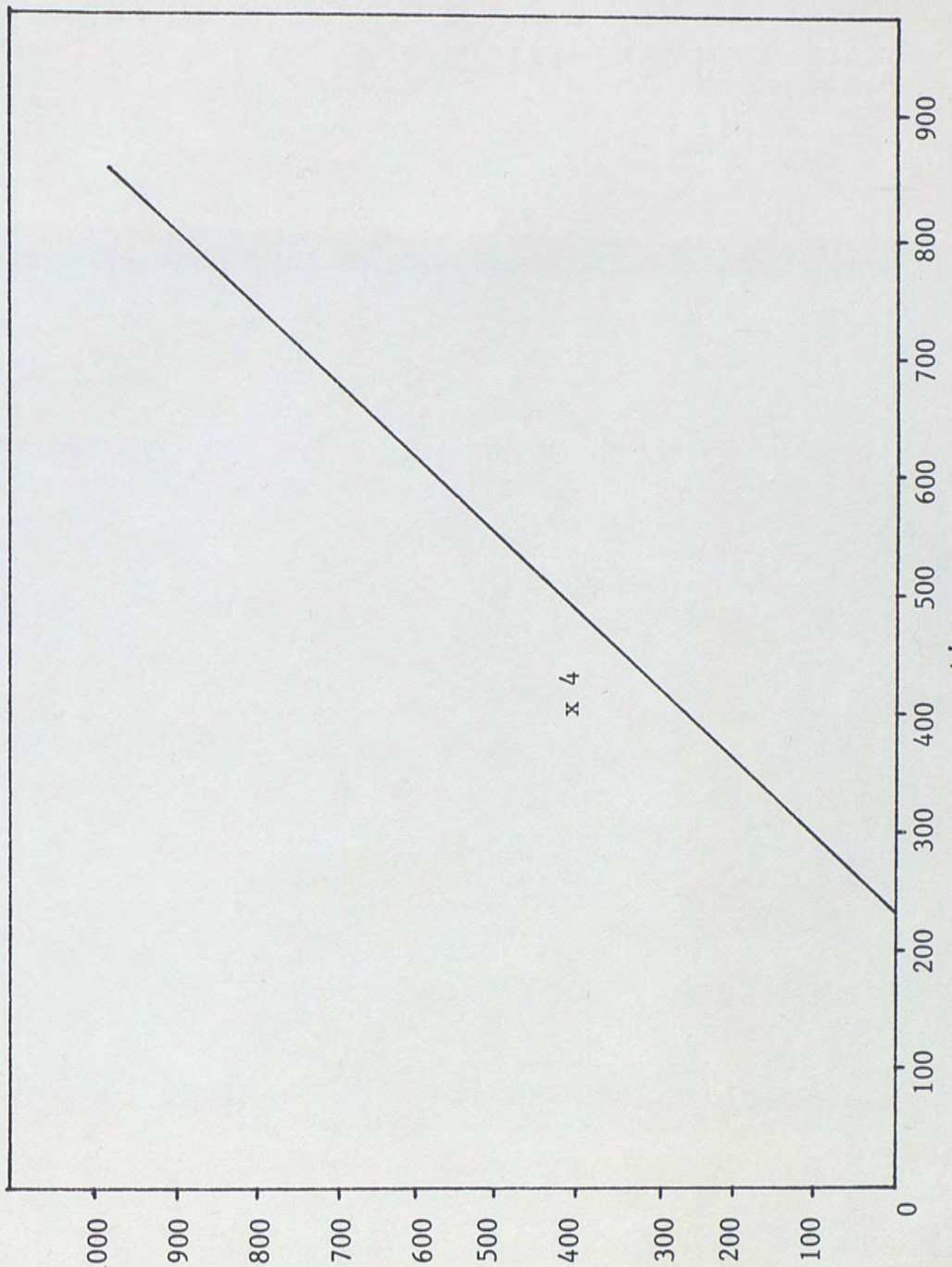

Fig. 33. Ultimate range calibration chart.

REFERENCES

Cook, John C. "Status of Ground Penetrating Radar and Some Recent Experience." In Subsurface Exploration for Underground Excavation and Heavy Construction. New York: American Society of Civil Engineers, 1974, pp. 175-194.

Cook, John C. "Radar Transparencies of Mine and Tunnel Rocks." Geophysics 40 (October 1975): 865-895.

Cook, John C. "Radar and Seismic Tunnel-Locating Techniques." Paper presented at the Symposium on Tunnel Detection. Colorado School of Mines. Golden, Colorado, July 21-23, 1981.

Dolphin, L.T.; Beatty, W.B.; and Tanzi, J.D. "Radar Probing of Victorio Peak, New Mexico." Geophysics 43 (December 1978): 1441-1448.

Doolittle, James A. Soils - Ground Penetrating Radar - Trip Report. Report by USDA Soil Conservation Service, File Code 430. Gainesville, Florida. October 1982.

Geophysical Survey Systems, Inc. Operating Manual Subsurface Interface Radar. Hudson, NH: Geophysical Survey Systems, Inc., 1982.

King, Ronald W.P., and Harrison, Charles W., Jr. "The Transmission of Electromagnetic Waves and Pulses into the Earth." Journal of Applied Physics 39 (August 1968): 4444-4452.

Kraichmann, M.B. Handbook of Electromagnetic Propagation in Conducting Media. Washington, D.C.: U.S. Government Printing Office, 1970 (Document NAVMAT, p. 2302).

Moffat, David L., and Puskar, R.J. "A Subsurface Electromagnetic Pulse Radar." Geophysics 41 (June 1976): 506-518.

Morey, Rexford M. "Continuous Subsurface Profiling by Impulse Radar." In Subsurface Exploration for Underground Excavation and Heavy Construction. New York: American Society of Civil Engineers, 1974, pp. 175-194.

Owen, Thomas E. "Cavity Detection Using VHF Hole-to-Hole Electromagnetic Techniques." Paper presented at Symposium on Tunnel Detection. Colorado School of Mines. Golden, Colorado, July 21-23, 1981.

Suhler, Sidney A. "Development of a Prototype Borehole Radar Probe." Paper presented at Symposium on Tunnel Detection. Colorado School of Mines. Golden, Colorado, July 21-23, 1981.

Ulriksen, C. Peter F. "Application of Impulse Radar to Civil Engineering." Dissertation, Lund University of Technology, Lund, Sweden, 1982.

Von Hippel, A.R. Dielectric Materials and Applications. New York: John Wiley and Sons, 1954.

Waite, J.R., ed. Electromagnetic Probing in Geophysics. Boulder, CO: The Golem Press, 1971.